

Answers to Reviewer #1:

General comments

We thank the reviewer for reviewing our paper. In the opening statement, the reviewer highlights that our paper contains interesting analysis with the potential for making an important contribution. At the same time, it is stated that the paper contains serious weaknesses, In particular the presentation is chaotic and often poorly worded. We do not agree with these last two statements. The presentation is not poorly worded. The presentation is systematic, not chaotic.

We have changed parts of the presentation and changed some wording to meet this criticism as is documented below. We note that the scientific content as such was not seriously questioned. We were a bit confused by the reviewers statement: The paper includes many unnecessary descriptive details that obscure important results and analysis (sic) that fails to adequately support the conclusions drawn from it.

Section 3.1.2. This section is considered too chaotic: (We assume that this is not meant to mean that a chaotic section would have been acceptable). We have changed this section throughout. When however the reviewer writes some conclusions seem overly speculative at least one example should have been given. We do not agree with the reviewer on this.

Section 3.1.3. This section contains far too many descriptive details: We have removed as many descriptive details as the order of argument allows for. Unfortunately, the reviewer does not even give one example of a descriptive detail that is not needed (out of the far too many).

Section 3.2. The section could be more meaningful showing statistics in Fig. 9 and 10: Adding more than one flight to Fig. 9 (now Fig. 10 in revised manuscript) would overcrowd the plot with too many coloured lines. It was already split in two panels to avoid this kind of overcrowding. However, we have changed Fig. 10 (now Fig. 11) to show source region statistics for all flights including panels showing the month-to-month variability. We have also followed the suggestion of Reviewer #2 to consider all trajectory points below 5 km instead of only the first time the trajectory reaches the lower troposphere.

Section 3.3.1. The reviewer writes ..this section could be deleted with no loss to the integrity or impact of the paper: We do not agree. Section 3.3.1. is a short subsection of Sect. 3 and deals by means of forward trajectories with the outflow of air from the UTAC for the locations for which we have measurement data. There are relatively few aircraft observation in the South Asian Summer Monsoon. The logic of this paper is to use our aircraft observations in relation to the trapping, chemistry and export. Surely, a valid question pertains to the outflow of this air. A focus for current research is the pathway of air from the regions involved into the stratosphere. We show by means of meteorological analyses where air from the UTAC is transported to. Its degree of dilution and the composition of the diluting air masses are not extractable from our data and only accessible at the moment by modeling. It would be a shame to delete this brief section from the paper. The decrease in impact would well surpass the decrease in size. We note, talking about impact, that the review spent most words on this section. We reiterate, it is at least of general interest to atmospheric chemists to know to where pollution that has been accumulated/trapped in the UTAC is exported.

The criterion for determining the influence of air along the flight path in receptor regions is imprecise and subject to severe sampling problems: We do NOT deal in this section with the influence of air in receptor regions. Therefore this statement in the review is void. We have, however, modified the text to mention that monsoon pollution export is not the only source of pollutants for the source regions and that its influence diminishes the further away the source region is from the monsoon UTAC.

The analysis in this section is weak: It must be clear that we deal here with a short subsection on the export regions. We cannot go further, and that may make the contents of this section weak in a quantitative sense. There are papers in the literature (e.g. *Scheeren et al., Atmos. Chem. Phys., 3(5), 15891608, 2003*) that deal with the impact of pollution transported from the UTAC elsewhere.

Section 3.3.2. The reviewer states. A cynical reviewer would wonder if the sampling and analysis criteria were chosen to provide the answer that the authors wanted rather than physically meaningful results: We find this an unworthy statement, even when anonymous. We expect facts in a valid review. Our reply: This section deals with the age of air masses, which is a complex concept. Two very different approaches are compared. One is that of a chemical clock based on NMHC ratios. Here a main a priori uncertainty is the choice of the amount of OH in the air masses. We justify this choice clearly (Spivakovskys OH distribution). The other one is that of trajectory calculations. Here a main a priori uncertainty is the starting point of the trajectories. We have now added a new Table 3 which lists the slopes of the least-squares fits for the correlations using start longitudes between 80°E and 100°E. We have changed the description of the results in the revised manuscript to: For July, the best fit was found when comparing the time since the air had last been east of 95°E. For August, the correlations do not change much for a source region between 85°E and 95°E. Concerning the sampling, we had already mentioned in the methods section that air samples were only collected during the first two flights in each month to achieve a better spatial resolution given the fixed number of 28 available air samples per month. We have repeated this in the beginning of this section and explained that consistent NMHC photochemical ages could not be calculated for the June and September samples. Therefore we are restricted to the samples from July and August. At the same time, these months represent the core of the monsoon period in India. The remaining 40 % of this section is used to discuss the problems of the two approaches.

Section 3.3.3. The reviewer writes: This section seems disconnected from the rest of the paper: As we outline above, and as the title of the paper communicates, this paper is about the trapping, chemistry and export of trace gases in the South Asian Summer Monsoon. This very section Monsoon UTAC leak rates deals with the escape of air from the UTAC. Estimates for a residence time of air in the UTAC are very useful and form an intrinsic part of this paper.

Specific Comments

Page 3, line 12. The word remarkable is too subjective and inappropriate and should be deleted throughout: The word remarkable had been used only thrice in the old manuscript and is now only used here in the abstract to highlight the consistency of a feature over 3500 km over the entire monsoon period for a range of trace gases. We adopt the suggestion by the reviewer about the consistent north-south gradient.

Page 11, line 12: We refer now to *Randel and Park, J. Geophys. Res., 111(D12), D12314, 2006*, and use the word suggested by the reviewer, namely interesting.

Page 11, lines 18-19: We now write: In general, the centre of the UTAC is observed to be furthest north during July (Fig. 4). This is consistent with meteorological studies of monsoon development, its northward propagation and recession (IMD, 2009).

Page 12, lines 13-16: As suggested, we have now changed the old Fig. 5 (now Fig. 6) to include data from all flights together with the means and the 1- σ standard deviations. The numbers for mean and standard deviation in the southern ($\Delta\text{lat } -7.5^\circ$ to -2.5°) and northern ($\Delta\text{lat } 2.5^\circ$ to 7.5°) section of the UTAC are now mentioned in the text. They show that there is a significant difference between the two sections except for CO which has its maximum around $\Delta\text{lat } -3^\circ$ and decreases both northwards and southwards.

Page 13, lines 1-7: It is well known that CO mixing ratios are higher in the troposphere than in the stratosphere and vice versa for O₃. Therefore in-mixing of stratospheric air would also lead to an increase of O₃ and a decrease of CO mixing ratios. The trajectories and NMHC ages both show that the air has been transported for a longer time since it was loaded with pollutants when we measure it in the northern part of the UTAC compared to its southern part. We also discuss the difference in nucleation mode particle number concentrations in the Supplement Sect. S5. We therefore do not understand well where the speculative part is.

Page 13, lines 7-9: We have now added the thresholds used for this filtering, namely 1.3 PVU and 150 ppb. The filtering has been done in the same way as for our previous monsoon studies by *Schuck et al. (2010)* and *Baker et al. (2011)*.

Page 13, lines 9-10: We have changed this to The distinction between freshly polluted air in the southern section and more processed, aged air in the northern section is also supported by a previous study of CARIBIC NMHC data (Baker et al., 2011).

Page 14, lines 3-11. Please explain (briefly) why positive correlations indicate ozone formation... We refer on page 14, line 5 to the paper by *Fishman and Crutzen (1978)*. Later we refer to other papers on ozone trends. This all is sufficient for a paper in an atmospheric chemistry journal. We have changed the wording to Positive correlations.

Figure 8: We have added the mean and 1- σ standard deviation to the plot. They support the C-shaped profile for CO, the decrease of water vapour with height and the increase of the aerosol particle concentrations with height. In the case of O₃, the increase with altitude from 4 km to 12 km is at the limit of significance, i.e. the upper bound at 4 km is only slightly lower than the lower bound at 12 km. If we were to use the patterns or trends quantitatively, we would have done more statistical analyses. However, the main features are clear in Figures 8 and 5 (now Figures 9 and 6 in the revised text).

Page 16, line 29 to Page 17, line 7: No, the C-shape is a typical vertical profile structure. It is like someone smoking a cigar in a room. We see smoke near the person and we see smoke higher up in the room (often stratified). We thus see a C-shaped profile. This is basically due to an observational bias, because the pollution at higher levels in the room has passed in a fairly

narrow single vertical corridor at relatively high speed to the higher level (see e.g. Fig. 2 in Barret *et al.*, *Atmos. Chem. Phys. Discuss.*, doi:10.5194/acp-2015-1011). In aircraft observations in the troposphere we have a similar effect. It is noteworthy that pilots do not wish to fly in the region where the pollution from below is transported rapidly upwards (e.g. inside thunderstorms).

Page 19, line 7: The choice of 5 km is arbitrary, but it is a sensible choice. We have repeated the calculations for 3 km and 1 km altitude and obtained very similar results. This is now mentioned more explicitly in the text together with an interpretation of this fact, namely that there must be rapid more or less directly vertical transport. The reliability of backward trajectories close to the surface is generally considerably less than backward trajectories in the free atmosphere. For the question where had the pollution been picked up the choice of 5 km is reasonable.

Page 25, lines 19-20: The proposed word reduced is unsuitable. Reduced means that a quantity is lesser than in a previous state. This does not apply here. We deal here with a vertical distribution pattern with higher mixing ratios at those levels where the outflow peaks and where dispersion over matter of days is less. We have changed the formulation to make it clearer. See above for an explanation of the higher pollutant levels above than below.

Page 25, lines 23-24: We have changed the formulation as it was indeed not clear.

Page 25, line 26 to Page 26, line 2: The statement by the reviewer **for example, it could be interpreted as saying that limiting the number of chemical species observed is expected to make a data set less consistent** is not correct. We have reformulated this part.

Page 27, lines 16-26: We disagree that this paragraph makes no logical sense. For clarification we have added at the end of this paragraph: In other words, the difference between the two regimes is due to the time elapsed since fresh pollution was injected into the UTAC.

Page 28, lines 12-13: Colleagues from other research institutions when dealing with the Asian Monsoon have introduced the concept trapping. In the current tone of reviewing the reviewer would point out that the air is not trapped, but escapes. So, this concept that is in use now would have been rejected. Meteorologists have used the concepts like Meteorological bomb (not rejected) or Stratospheric fountain (not rejected) and we used merry go around (hopefully not ejected). As long as humans do science and it is communicated in language not all qualifiers will be perfect descriptors.

Page 28, lines 16-24: The reviewer is mistaken. It does not refer to an artifact of the flight path.

Page 28, lines 26-27: We have removed this piece of information.

Selected technical details

We have incorporated the changes suggested by the reviewer. Please see the revised manuscript and the track-changes version for details.

Answers to Reviewer #2:

We would like to thank referee #2 for his thorough review of our manuscript and his helpful suggestions for improving the manuscript. In the following, we will answer his specific comments.

General remarks

The reviewer makes two main points. One is that more information on the emissions should be given. Therefore we now have included plots of emission distributions from the Regional Emission inventory in ASia (REAS) version 2.1 for CO and the sum of all non-methane volatile organic compounds (NMVOC) for India and the surrounding region for August 2008 as a new Figure 2. A complete emission inventory is beyond the scope of our paper. In the meantime a modeling paper on CO emissions and a comparison of CO and O₃ with the CARIBIC data has been published (*Ohja et al., Atmos. Chem. Phys. Discuss., 15(15), 2113321176, 2015*).

The second point is that although convection and scavenging are often referred to, neither vertical wind speeds nor precipitation patterns are part of the meteorological parameters described. We indeed referred often to convection but did not give vertical wind data. We rather have indicated the general feature of the strongest convection being over the Bay of Bengal. For a more detailed link between observed pollution and convection one indeed needs the emission distribution. In the case of convection a detailed analysis of the measurements along the flight track would need to be made in comparison to the meteorological data. One would need to have a map of the true location and strength of all convective cells, the emissions from the inventory and the trajectories, which themselves again are dependent on knowing the exact distribution of the convection (which in the FLEXPART trajectory model is parameterized using meteorological information from ECMWF at 1° × 1° spacial resolution which is not resolving the single convective cells). We consider the amount of chemical measurement data not sufficient for justifying such a study and the detailed knowledge about the convection hard to get. Such work is more within the realms of dedicated measurement campaigns and research aircraft. Similarly, we argue that scavenging studies are likewise too detailed for the dataset we have. The very short lifetimes of scavenged species, e.g. the nucleation mode aerosol particles N_{4–12} in Figure 6E (in the revised manuscript) (which also are formed rapidly) show the complexity of linking precipitation with our data in detail. In addition we discuss the differences of the nucleation mode aerosol particle concentrations N_{4–12} in the northern and southern part of the UTAC in the supplement (Sect. S5 and Figs S23 & S24).

Other comments

p 972 line 7: Our description was incomplete, we now have remedied this.

p 6973 line 20: We now have added more information on the wind field in the revised manuscript.

p 6975 line 27: We are interested in the air mass origin along the flight track. Therefore we start many single trajectories/particles along the flight track and track the particle/trajectory position instead of releasing many particles from one point along the flight track and calculating the footprint for this one single point.

p 6979 line 9: As in the previous studies by *Schuck et al. (2010)* and *Baker et al. (2011)*, we

used thresholds of 1.3 PVU and 150 ppb for PV and ozone, respectively. These numbers have been added to the text.

p 6979 line 15: We have added mean numbers and variabilities when describing the revised version of Fig. 6.

p 6981 line 27: Figure 1 has already a high density of information and this information is for 250 hPa and not the lower level of the Somali jet (which has its maximum around 850 hPa). We would need another more general figure for the overall meteorological description, including the Somali Jet. Instead we refer to *Chakraborty et al., Int. J. Climatol., 29, 983992, 2009*, for a study showing the horizontal and vertical extent of the Somali Jet.

p 6985 line 7: Reviewer #1 made a similar point. We also have used levels below 5 km but it makes little difference. We have now used all points below the 5 km threshold for creating the source region distribution plots in Fig. 11 in the revised manuscript. It now shows the mean distribution together with its month-to-month variability. We do not quantify the amount of boundary layer air that had become entrained rather us this simple approach.

p 6989 line 19: Figure 16 shows that more and more trajectories join the UTAC in the 10 days prior to the flight and that they leave the UTAC again, indicative of leaking. The fraction of trajectories in the UTAC increases from 60–70 % 10 days before the flight to 100 % (by definition) at the flight and then decreases again to 30–50 % 10 days after the flight. We modified the text.

p 6991 line 17: We have changed the formulation

p 6992 line 24: We have changed the formulation

Figure 9 (now 10): The starting points of the trajectory are now marked with black dots.

Figure 9b (now 10b): Fig. 11 in the revised manuscript shows that the source regions are rather split north-east / south-west for the northern and the southern section of the UTAC. In that respect, our relative latitude coordinate already divides the measurements by source region (e.g. in Figs. 6, 7, 14 & 15).

Figure 11, 12: We agree that to estimate the impact of the monsoon air on a receptor region, one needs to work backwards from the receptor region to find out how big the influence of the monsoon is. However, we find it still instructive to see where and how far the monsoon air can be transported in certain cases. So even when sampling air over the eastern coast of Canada, one should keep in mind that it may be influenced by the monsoon (see North America receptor region and our CARIBIC observations in September 2007 described in the Supplement Sect. S1). Therefore we would like to keep this section in the main text. We have added some text discussion the issue of influence on the receptor region.

Technical comments

Abbreviations: This has been corrected unless the abbreviation would stand in the beginning of a sentence.

3.1.1 in the heading maybe add aircraft or measurement position is: Heading has been changed to Measurement position in ...

p 6978 line 4: which flight in August - add date: The date (14 August 2008) has been added.

p 6982 line 16: write Fig 8b instead of Panel B - makes it better readable: This has been changed in the whole manuscript not only for Fig. 8.

Trapping, chemistry and export of trace gases in the South Asian summer monsoon observed during CARIBIC flights in 2008

A. Rauthe-Schöch¹, A. K. Baker¹, T. J. Schuck^{1,*}, C. A. M. Brenninkmeijer¹, A. Zahn², M. Hermann³, G. Stratmann⁴, H. Ziereis⁴, P. F. J. van Velthoven⁵, and J. Lelieveld¹

¹Max Planck Institute for Chemistry (Otto Hahn Institute), Department of Atmospheric Chemistry, Mainz, Germany

²Karlsruhe Institute of Technology (KIT), Institute for Meteorology and Climate Research, Karlsruhe, Germany

³Leibniz Institute for Tropospheric Research (TROPOS), Leipzig, Germany

⁴German Aerospace Center (DLR), Institute for Atmospheric Physics, Oberpfaffenhofen, Germany

⁵Royal Netherlands Meteorological Institute (KNMI), De Bilt, the Netherlands

* now at Goethe University Frankfurt, Institute for Atmospheric and Environmental Sciences, Frankfurt/Main, Germany

Correspondence to: A. Rauthe-Schöch (armin.rauthe-schoech@mpic.de)

Abstract. The CARIBIC (Civil Aircraft for the Regular Investigation of the Atmosphere Based on an Instrument Container) passenger aircraft observatory performed in situ measurements at 10–12 km altitude in the South Asian summer monsoon anticyclone between June and September 2008. These measurements enable us to investigate this atmospheric region ~~;~~ (which so far has mostly been observed from satellites~~;~~) using the broad suite of trace gases and aerosols measured by CARIBIC.

5 Elevated levels of a range-variety of atmospheric pollutants ~~were recorded~~ (e.g. carbon monoxide, total reactive nitrogen oxides, aerosol particles and several volatile organic compounds) were recorded. The measurements provide detailed information about the chemical composition of air in different parts of the monsoon anticyclone, particularly of ozone precursors. While covering a range of 3500 km inside the monsoon anticyclone, CARIBIC observations show remarkable consistency, i.e. with regular distinct latitudinal patterns of trace gases during the entire monsoon period. ~~Trajectory calculations indicate that these air~~
10 ~~masses originated mainly from South Asia and Mainland Southeast Asia.~~

Using the CARIBIC trace gas and aerosol measurements in combination with the Lagrangian particle dispersion model FLEXPART we investigated the characteristics of monsoon outflow and the chemical evolution of air masses during transport.

The trajectory calculations indicate that these air masses originated mainly from South Asia and Mainland Southeast Asia.

Estimated photochemical ages of the air were found to agree well with transport times from a source region east of 95⁹⁰–95° E.

15 The photochemical ages of the air in the southern part of the monsoon anticyclone were consistently-systematically younger (less than 7 days) and the air masses were mostly in an ozone forming chemical regimemode. In its northern part the air masses were older (up to 13 days) and had unclear ozone formation or destruction potential. Based on analysis of forward trajectories several receptor regions were identified. In addition to predominantly westward transport, we found evidence for
20 tropopause exchange, which was strongest during June and July. Westward transport to Africa and further to the Mediterranean was the main pathway during July.

1 Introduction

During boreal summer the South Asian monsoon dominates atmospheric circulation over Asia, and has a strong influence on atmospheric transport and chemistry of ~~most~~ much of the northern hemisphere (Randel and Jensen, 2013). The monsoon is characterised by a persistent large-scale anticyclonic structure in the upper troposphere, centred over Pakistan and Northern India, framed by the subtropical eastward jet in the north and ~~the a~~ westward equatorial jet in the south. This upper troposphere anticyclone (UTAC) is not static but oscillates in strength, shape and position (Garny and Randel, 2013). At the same time it features a ~~remarkably~~ strikingly distinct composition signature throughout the monsoon season. Observations from satellites have shown an enhancement of mixing ratios of a number of trace gases in the UTAC, most prominently methane (CH₄) (Xiong et al., 2009) and carbon monoxide (CO) (Kar et al., 2004). Since the monsoon is accompanied by strong convection, upper tropospheric trace gas mixing ratios are directly linked to surface emissions in this densely populated region. In addition, polluted air masses can be trapped and accumulate inside the UTAC, where they can be chemically isolated for several days (Randel and Park, 2006; Park et al., 2008). The UTAC can also play a governing role in the dispersion of volcanic plumes, e.g. after the June 2011 eruption of the Nabro volcano in Eritrea (Fairlie et al., 2014). Outflow occurs predominantly westward towards Northern Africa and the Middle East, where a summertime ozone (O₃) maximum due to ozone formation in monsoon outflow has been reported (Li et al., 2001; Liu et al., 2009), and to the Mediterranean region (Lelieveld et al., 2002; Scheeren et al., 2003). Not only does the South Asian summer monsoon influence ~~the composition of the~~ trace gas and aerosol particle loadings in the upper troposphere, it also affects cross-tropopause transport into the lowermost stratosphere (Traub and Lelieveld, 2003; Lelieveld et al., 2007; Randel et al., 2010; Chen et al., 2012). An extensive review on southern Asian pollution outflow in all seasons is given by Lawrence and Lelieveld (2010).

While most observations in the South Asian summer monsoon UTAC are from satellites, CARIBIC (Civil Aircraft for the Regular Investigation of the Atmosphere Based on an Instrument Container, www.caribic-atmospheric.com, Brenninkmeijer et al., 2007) phase 2 provides ~~the~~ first in situ observations over the Indian subcontinent, performed during the 2008 monsoon season. During the summer monsoon period from June through September, 14 flights between Frankfurt, Germany and Chennai, India, were conducted, crossing the western part of the UTAC at altitudes between 10 and 12 km. The CARIBIC observatory thus ~~provided the comprehensive~~ contributes to the measurements within the UTAC called for by experts on atmospheric chemistry and the Asian monsoon (Crawford and Pan, 2013; Pan et al., 2014). The CARIBIC in situ observations in the upper troposphere aim to contribute to the understanding of the monsoon and its impacts on atmospheric composition ~~through this~~ through this work and previous studies ~~-~~

~~Elevated~~ which dealt with the elevated mixing ratios of a range of trace gases ~~were measured~~ that were measured by CARIBIC within the UTAC, for example CO, CH₄, nitrous oxide (N₂O), sulfur hexafluoride (SF₆) (Schuck et al., 2010), several non-methane hydrocarbons (NMHCs, Baker et al., 2011) as well as methyl chloride (CH₃Cl, Umezawa et al., 2014, 2015). Furthermore, as earlier measurements from CARIBIC phase 1 have shown, aerosol particle number concentrations are enhanced in the UTAC (Hermann et al., 2003). Trajectory calculations indicated that the air masses originated mainly from South Asia and Mainland Southeast Asia and had been transported up to cruise altitude by deep convection associated with the

summer monsoon. High mixing ratios of water vapour at southern latitudes confirmed that recent convection had occurred. An analysis of tracer correlations, namely CO, CH₄ and ethane (C₂H₆), revealed that, in addition to enhanced vertical transport of polluted boundary layer air, emissions of methane from biogenic sources, such as wetlands, open landfills, and rice paddies, increase during the summer months (Baker et al., 2012), resulting in disproportionately high mixing ratios. Carbon dioxide (CO₂) mixing ratios were found to be lower inside the UTAC. A model study using CARIBIC data found that, at least in 2008, the region was a net sink of CO₂ because of strong uptake by the terrestrial biosphere (Patra et al., 2011). ~~Additionally, Independently, observed low CO₂ mixing ratios with increased $\delta^{13}\text{C}(\text{CO}_2)$ values combined with low $\delta^{18}\text{O}(\text{CO}_2)$ values indicate oxygen-photosynthetic uptake of CO₂ and oxygen atom exchange with soil and leaf water (Assonov et al., 2010).~~

~~In September 2007~~ Interestingly, the CARIBIC aircraft observatory also encountered air masses with the typical monsoon signature of elevated mixing ratios of CH₄, N₂O, SF₆ and some NMHCs, accompanied by relatively low CO₂ mixing ratios. ~~In this case it was not over far away from~~ the South Asian monsoon region, ~~but namely~~ over eastern Canada in the vicinity of Toronto in September 2007. This raises the question about the whereabouts of air masses that are exported from the UTAC. Air mass trajectories pointed to export from the monsoon region (see Sect. S1 for details), although transport of Asian pollution over the Pacific towards North America occurs predominantly in the northern hemispheric winter and spring (Liu et al., 2003) whereas in summer westward outflow is prevalent. While no comparable case was observed during CARIBIC flights to North America in subsequent years, plumes of photochemically processed air originating from Asia have been probed over different parts of North America during INTEX-NA (The Intercontinental Chemical Transport Experiment – North America) flights in July and August 2004 (Liang et al., 2007).

CARIBIC measurements yield a fairly detailed description of the chemical composition of air in different parts of the UTAC, including mixing ratios of ozone precursors like the sum of reactive nitrogen oxides (NO_y), CO and NMHCs. Using this information and the Lagrangian particle dispersion model FLEXPART (Stohl et al., 2005) we investigate the characteristics of ~~monsoon outflow and the chemical evolution of air masses during transport. Based on analysis the trapping of pollution, its distribution and the evolution of chemical composition in the UTAC. Furthermore, based on analyses of~~ air mass forward trajectories several receptor regions are identified and their relative role for monsoon pollution export is tentatively quantified. Additional material is presented in the supplement.

2 Methods

The CARIBIC observatory phase 2 started ~~routine operation in 2005. It is operates on a monthly basis aboard a its routine operation, using a~~ Lufthansa Airbus A340-600 to make ~~observations during a series of two to six measurements during sequences of typically four~~ long distance flights. ~~The aircraft is fitted per month, in 2005. This specific aircraft was retro-fitted in 2004~~ with a permanently mounted air and aerosol particle inlet system which is connected via (partially heated) stainless steel tubing ~~to the CARIBIC container when installed. Some of the tubings are lined with thin-walled PFA tubes to avoid wall effects (some of which lined with perfluoroalkoxy alkane (PFA) to reduce wall effects) to the CARIBIC container when installed~~ (Brennkmeijer et al., 2007). The 1.6 ton container houses instruments for in situ measurements and remote sensing

as well as ~~glass flasks for the collection of whole air samples~~ systems for air and aerosol particle collection. In this study results from both the in situ measurements providing a high data density along the flight track, and from the air sampling equipment are used. The latter gives a low data density (28 samples per monthly flight sequence) but with more details because many more trace gases are analysed retrospectively in the collected air samples. Flights start from Frankfurt (since August 2014 from Munich), Germany, to various destinations around the globe. After the final return flight, the container is unloaded, the measurement data are retrieved and the air samples are analysed for a suite of different trace gases in several laboratories (Brenninkmeijer et al., 2007; Schuck et al., 2009; Baker et al., 2010; O’Sullivan, 2007).

From April to December 2008, the CARIBIC container ~~measured took measurements~~ during 32 flights between Frankfurt, Germany and Chennai, India (see list on www.caribic-atmospheric.com). For this study, we consider ~~only~~ the 14 “monsoon” flights conducted between June and September 2008 (see list of flights in Table 1). These months represent the core of the monsoon period over India ~~in this year~~ as previously discussed by Schuck et al. (2010) and Baker et al. (2011). More information about the non-monsoon months can be found in these two previous studies and will not be discussed here. All 14 flights crossed the western part of the monsoon UTAC ~~over between~~ the western coast of India ~~before reaching and~~ Chennai at the ~~east southeast~~ coast. The UTAC was probed at altitudes between 10.3 and 11.9 km (see Fig. S4). ~~ECMWF winds~~ Wind fields obtained from the European Centre for Medium-Range Weather Forecasts (ECMWF) at the 250 hPa model level, which corresponds approximately to the flight altitude, are shown as 10-day means in Fig. 1. In the north, the meandering sub-tropical jet is shifted northwards and slows down as the monsoon progresses northwards from June to August while it regains strength and moves south in September as the monsoon retreats. In June, the wind arrows show the UTAC centred over northern India and Pakistan. July shows an expansion of the UTAC towards eastern China and a split of the UTAC with a second “eye” over northern Africa. In August, the centre of the UTAC is spread out over northern India, Pakistan and the Arabian peninsula and with the retreat of the monsoon in September, the UTAC slowly fades and is less clearly visible in the wind field.

In addition to a suitable wind field structure provided by the monsoon UTAC, trapping pollutants also requires sources for these which are typically located at the ground (e.g. Vogel et al., 2015). Figure 2 shows emission data for CO and the sum of all non-methane volatile organic compounds (NMVOC) from all sources listed in the Regional Emission inventory in ASia (REAS) version 2.1 (Kurokawa et al., 2013, including the November 2013 update) for August 2008 in India and the surrounding region below the UTAC and in its source region. The geographical distributions for CO (left panel) and NMVOC (right panel) are similar in the region. The Indo-Gangetic plain in northern India and South Central China show high CO emissions together with parts of Thailand and Vietnam. NMVOC emissions are somewhat higher in southern India and lower in South Central China compared to CO emissions. Detailed modelling studies with the Weather Research and Forecasting with Chemistry (WRFChem) online regional chemistry transport model to link emissions and transport have been published separately (Ojha et al., 2015).

2.1 CARIBIC trace gas and aerosol measurements

The CARIBIC container houses a number of different instruments for measuring ~~various trace gases as well as a spectrum of trace gases and also~~ aerosol particles (Brenninkmeijer et al., 2007). Discussed extensively in this work are ~~carbon monoxide~~

~~(CO), ozone (O₃), the sum of reactive nitrogen oxides (NO_y), CO, O₃, NO_y~~ and aerosol particles (N_{4–12} and N₁₂). Brief descriptions of these measurements are presented next.

~~CO~~ Carbon monoxide is measured with an AeroLaser AL 5002 resonance fluorescence UV instrument modified for use on-board the CARIBIC passenger aircraft. ~~Alterations were necessary to optimise the instrument reliability to allow for automated operation over an entire CARIBIC flight sequence lasting several days.~~ The instrument has a precision of 1–2 ppbv at an integration time of 1 s and performs an in-flight calibration every 25 min. A technical description of the CO instrument can be found in Scharffe et al. (2012).

~~The ozone measurement is~~ Ozone measurements are based on a fast, commercially available dry chemiluminescence (CL) instrument, which at typical ozone mixing ratios between 10 ppbv and 100 ppbv and a measurement frequency of 10 Hz has a precision of 0.3–1.0 %. The performance of this instrument has been characterised in detail by Zahn et al. (2012). The absolute ozone concentration is inferred from a UV-photometer designed in-house which operates at 0.25 Hz and reaches an accuracy of 0.5 ppbv. ~~The CL instrument has been characterised in detail by—~~

The sum of reactive nitrogen oxides (NO_y) is ~~detected using a two-channel NO monitor where chemiluminescence detection is used with NO_y being measured after catalytic conversion~~ determined using an NO chemiluminescence detector (Eco Physics AG) after conversion of NO_y to NO (Ziereis et al., 2000). The time resolution is ~~also~~ 1 s. The overall uncertainty for the NO_y measurement at 10 s time resolution is about 7 % at 450 pptv NO_y (Brough et al., 2003).

The total water mixing ratio (gaseous, liquid and ice phase) is measured by means of a chilled mirror frost-point hygrometer (CR-2, Buck Research Instruments L.L.C.) with a time resolution of 5 (high humidity) to 300 s in the dry lowermost stratosphere with an uncertainty of around 0.3 ppmv at cruise altitude. A modified two-channel photo-acoustic diode-laser spectrometer (Hilase, Hungary) measures both gaseous (H₂O_{gas}) and total water mixing ratios with a time resolution of 3 s and a precision of 1 ppmv. These measurements are calibrated to the absolute water mixing ratios determined with the frost-point hygrometer. A detailed description of the CARIBIC humidity measurements is available in Dyroff et al. (2015). An overview of the H₂O data has been published by Zahn et al. (2014).

Integral aerosol particle number concentrations are measured with three condensation particle counters (CPC, modified TSI model 7610) with lower threshold diameters (50 % counting efficiency) of 4, 12 and 18 nm, respectively, and an upper detection limit of around 2 μm at 200 hPa operating pressure (Hermann and Wiedensohler, 2001). The difference ~~of in counts between~~ the 4 and 12 nm channels is called given as N_{4–12} and corresponds to the nucleation mode. The 12 nm channel (N₁₂) corresponds ~~mainly to the Aitken mode~~ in the upper troposphere where the CARIBIC aircraft is taking measurements mainly to the Aitken mode. All aerosol particle number concentrations used in this paper are given at standard pressure and temperature (STP) of 273.15 K, 1013.25 hPa.

Whole air samples are collected in two units, each of which contains 14 glass sampling flasks of 2.7 L volume, pressurised to ~4.5 bar during collection. Samples were collected at pre-determined, evenly spaced intervals of roughly 35 min (~480 km) with filling times between 0.5 and 1.5 min (~7–22 km). In months with four flights between Frankfurt and Chennai, i.e. June, August and September 2008, sample collection only took place during the first two flights in order to achieve higher spatial and temporal resolution (see last column in Table 1). Greenhouse gases ~~and non-methane hydrocarbons (NMHCs) are~~ (GHGs)

and NMHCs were measured post-flight in the laboratory at the Max Planck Institute for Chemistry in Mainz using separate Germany. GHGs are separated with a gas chromatography (GC) systems coupling GC separation with system and then measured by flame ionisation detection (GC-FID) or CO₂ and CH₄ and electron capture detection (GC-ECD) ECD, N₂O and SF₆. Schuck et al., 2009), while the NMHCs are separated on a second GC system and then measured by ECD (Baker et al., 5 2010).

2.2 FLEXPART trajectory calculations

FLEXPART is a widely used Lagrangian particle dispersion model in ongoing development at the Norwegian Institute for Air Research (NILU) that in our case obtains its meteorological input data from the European Centre for Medium-Range Weather Forecasts (ECMWF). It simulates long-range and mesoscale transport, diffusion, dry and wet deposition, and radioactive decay of various tracers (see detailed description in Stohl et al., 2005). An updated description of the FLEXPART model is available from Stohl et al. (2010). In the current study, FLEXPART version 9.02 together with ECMWF meteorological input data with a temporal resolution of three hours and a spatial resolution of 1.0° × 1.0° and 91 model levels was used.

We started trajectories every 3 min along the flight tracks and calculated them 14 days forward and backward in the single trajectory mode of FLEXPART with enabled parameterisations for the sub-grid terrain effect and sub-grid convection. The trajectory positions were recorded every 30 min. The southernmost point of our flight track is Chennai (12.99° N, 80.18° E). The northern cut-offs for the trajectory analysis are 36.5° N in June, 40.0° N in July and August, and 35.5° N in September (see Table 1) and were chosen to exclude the subtropical jet stream and thus concentrate the analysis on the monsoon region. The continuous trace gas measurements were averaged over 60 s centred around the start points of the trajectories along the flight track to obtain representative trace gas concentrations for the air characterised by the trajectories.

20 3 Results and discussion

In the following, we We will first present the CARIBIC observations of trace gases and aerosol particles (Sect. 3.1.1) and with their latitudinal and photochemical distributions and characteristics (Sect. 3.1.2) before investigating the. The vertical profiles measured by CARIBIC over Chennai in are presented next (Sect. 3.1.3). Then we show the origins of these air masses (Sect. 3.2) and continue with a description of where the air is transported to after it has spent time in the monsoon upper 25 troposphere anticyclone (UTAC) UTAC and how long it remains trapped inside the UTAC it (Sect. 3.3).

3.1 CARIBIC observations

Here we present The following sections discuss the CARIBIC observations and what how the latitudinal and vertical variations in the trace gas mixing ratios tell us can be used to infer information about the chemical properties of the observed air masses and their origin.

3.1.1 ~~Position within~~ Measurement position in the upper troposphere anticyclone (UTAC)

Along routes between Chennai and Frankfurt during the monsoon season (June–September 2008) the aircraft passed from the southern section of the UTAC, where winds are from the east, through the centre into the northern section, where winds are from the west or vice versa for flights from Frankfurt to Chennai. The transition between the two regimes is evident in the wind data recorded by the aircraft ~~, with an abrupt change in wind direction observed (Fig. 3) which show abrupt wind direction reversals~~ in the vicinity of 26° N ~~(Fig. 3, note that 90 means wind from the east, 180 from the south, 270 from the west).~~ Wind speeds are low in the centre of the UTAC ~~, (reaching near zero at the transition point and increasing)~~ and increase strongly at the northern edge of the UTAC and upon entering the northern hemisphere subtropical jet stream ~~. The latitude where~~ (see also flight tracks in Fig. 1). The latitude at which the aircraft crosses between the two sections or regimes varies from month to month, with the northernmost average location in July and the southernmost in September (Figs. 3, 4 and Table 1). ~~There are also variations~~ It is noted that there are differences observed between flights in each single month, with the point of transition on the flights to Chennai being systematically further north than on the corresponding return flights. ~~This arises from the variations in flight altitude with~~ The systematic differences in altitude expose a vertical structure in the UTAC. The cruise altitudes of the aircraft at 22–28° N for flights to Chennai being at about are 1–2 km higher altitude than (since most aircraft fuel has already been burned) than during the return flights at the transition point ((when the aircrafts fuel tanks are still full shortly after take-off, see Fig. S4). ~~The flight routes themselves, however, did not change~~ However, the flight routes to and from Chennai between 22 and 30° N ~~from month to month for the forward and return flights for each month were identical~~ with the exception of one return flight in August (Fig. S5). ~~Therefore changes between months~~ This implies that the differences observed between individual months (at the same altitude ~~reflect changes in monsoon circulation~~) document changes in the structure of the monsoon circulation (in the horizontal and/or the vertical direction). The observed northwards shift of the UTAC centre at higher altitude means that we observe an interesting northward tilt of the monsoon axis, consistent with previous work (e.g. Randel and Park, 2006, their Fig. 2). In general, the centre of the UTAC is observed to be furthest north during July ~~, and this observation~~ (Fig. 4). This is consistent with meteorological studies of monsoon development, its northward propagation and recession (IMD, 2009).

~~In an effort to~~ To compensate for biases attributable to variations in flight routes and/or horizontal movements of the monsoon UTAC, and to normalise for position within the UTAC between months, ~~data are given~~ we give our data an additional latitudinal coordinate. Relative latitude (Δlat) ~~describes~~ defines the location relative to the latitude at which the aircraft crosses from the northern to the southern section of the UTAC or vice versa (i.e. relative to the “centre” of the UTAC indicated by the reversal of the zonal wind). Positive Δlat describes measurements in the north, negative Δlat measurements in the south, with values determined on a per flight basis.

3.1.2 Latitudinal transects

As ~~the aircraft moved from south to north we observed a distinct latitudinal structure in chemical tracers~~ an example for the UTAC being fully developed, Fig. 5 gives the individual trace gas, aerosol particles and wind latitude transect profiles for the

second flight from Frankfurt to Chennai in August (14 August 2008) at altitudes of 10.3 to 11.9 km between approximately 15–14 and 40° N, shown in Fig. 5 for a single flight in August, when the UTAC was fully developed. The southern section of the flight track (12–2814–25° N) is characterised by relatively low O₃ (panel A, Fig. 5A, average value 39 ppb for Δlat –7.5 to –2.5°), considering that the mean concentrations over all flights and lie between 51±11 (Δlat –7.5 to –2.5° of
5 51 vs.) and 81±13 ppb for (for the northern part, Δlat 2.5 to 7.5°) and NO_y (panel B, low NO_y (Fig. 5B, average value
0.33 ppb with corresponding mean concentrations of 0.56 vs. 0.810.57±0.38 and 0.83±25 ppb) and elevated concomitant with
high CO (panel A, Fig. 5A, average value 96 ppb with corresponding mean concentrations of 101 vs. ±8 and 92±10 ppb),
high water vapour (panel B, 390 vs. Fig. 5B, average value 299 ppm with corresponding mean concentrations of 409±219 and
35±41 ppm) and aerosol particles (panel high aerosol particle number concentrations (Fig. 5C). In the north (28–40 northern
10 section (27–40° N), the opposite is observed; mixing ratios of O₃ and NO_y are elevated, (average value 86 ppb for Δlat 2.5
to 7.5°) and NO_y (average value 0.81 ppb) are elevated while levels of CO decrease and especially are a little higher for this
flight (average value 102 ppb). Here especially the levels of water vapour and aerosol particle number concentrations are much
lower, with the exception of some brief instances of elevated nucleation mode (N_{4–12}) particle number concentrations. This
distinct pattern is observed during These distinct and clear patterns are observed for all flights under investigation in all months
15 and is are attributable to the influence of different air mass source regions, different chemical regimes and varying transport
times within the different regions of the UTAC (see Figs also Fig. 6 and S9–S24 below and Figs. S9–S21).

An important feature of the monsoon is persistent deep convection over South Asia, which is strongest over the Bay of Bengal and the Indian subcontinent (Devasthale and Fueglistaler, 2010). South of ~25~26° N (Δlat < 0) the aircraft encountered air that has had passed over these highly active convective regions and has had become burdened with emissions from South
20 Asia. This accounts for enhancements in the primary pollutant CO and relatively low levels of the secondary pollutant O₃, as
well as the enhancements in water vapour and. Likewise high levels of nucleation mode aerosol particles (i.e. freshly formed
particles, N_{4–12}) which can be regarded as tracers for convection and persisted. These aerosol particles are very short-lived
relative to the other species (hours to a few days) and can be regarded as indicators of convection (Weigelt et al., 2009)
Interestingly, mixing ratios of NO_y are lower in the south than in the north (0.37 ppb vs. 0.72 ppb), possibly as a result of
25 lower NO_x emissions in the south combined with the conversion to water soluble components of NO_y in the highly reactive
polluted air masses followed by enhanced removal under the high temperature, high humidity conditions of the monsoon. In
the north, the air parcels encountered by CARIBIC have been transported for longer periods of time several days within the
UTAC and show signs of chemical processing and aging. Water vapour and nucleation mode particles have been depleted by
experiencing cold low temperatures during transport and washout, respectively. CO levels are reduced and O₃, given more time
30 to form photochemically, is elevated. Similar changes in composition could have been caused by in-mixing of stratospheric air.
However care has been taken to identify and remove all data points that have stratospheric influence based on the measured
ozone concentrations and the potential vorticity (PV) values from the ECMWF model The results are supported by our
previous findings from measurements of NMHCs using thresholds of 150 ppb and 1.3 PVU for ozone and PV, respectively.
The distinction between freshly polluted air in the southern section and more processed, aged air in the northern section is also
35 supported by a previous study of CARIBIC NMHC data (Baker et al., 2011).

A comparison of the latitudinal profiles for the first return flight to Chennai during each month is shown. Results for all individual flights are plotted against relative latitude in Fig. 6. The standard deviation calculated over moving 2° relative latitude bins is shown as grey shading. Water vapour in Fig. 6A is shown on a logarithmic scale. The differences of the means for the southern and northern section of the flights are larger than the $1-\sigma$ standard deviation (see numbers given above) for all trace gases except for CO which shows a maximum slightly south of the wind reversal ($\Delta\text{lat} \sim 3^\circ$) decreasing southwards and northwards. Profiles for subsequent flights are shown in Figs. S22–S24. In general, trace gas (panels Fig. 6A–D) and aerosol particle (panels concentration (Fig. 6E and 6F) profiles in June, July, August and September are similar to those observed in August, although mixing ratios vary between the months, and in each month the overall pattern is interrupted by unique, although the overall patterns are interrupted by certain events. Notable features are the much higher NO_y (panel Fig. 6D) and lower CO (panel Fig. 6B) in the north during September (with no notable difference for O_3), and the abrupt gradient in CO concentrations between north and south during June. The large variability in aerosol particles compared to the trace gases is caused by the strong dependency of the particle number concentration on clouds whose position relative to the CARIBIC flight tracks was different during each flight. Monthly mean aerosol particle distributions by latitude are shown in Sect. S5. A detailed investigation of clouds and particle number densities is beyond the scope of this work and the interested reader is referred to the CARIBIC based work by Weigelt et al. (2009).

As our analysis focuses on the monsoon as a transport mechanism for polluted air masses from South Asia and Mainland Southeast Asia and the influence on other regions, understanding the composition and chemistry of air parcels as they move through the UTAC is critical in for evaluating the potential impact on downwind regions. This includes understanding not only of primary pollutants in transported air masses, but also of the tendency to form secondary pollutants, in particular ozone. Previous analysis particularly ozone. A previous CARIBIC data based study of the relationship between ozone and NMHCs, which are indicators of pollution and act to some degree as ozone precursors, has shown showed that air masses in the south have a greater ozone formation potential than in the north, where air masses have diminished formation potential or show the beginnings of ozone destruction (Baker et al., 2011). Ozone formation potentials in the troposphere can also be qualitatively understood through the relationship between ozone and carbon monoxide using the enhancement ratio $\Delta\text{O}_3/\Delta\text{CO}$ (Fishman and Crutzen, 1978; Parrish et al., 1998; Zahn et al., 2002), as determined from correlation plots, in addition to the information provided by the coarser resolution NMHC data. Positive slopes of the correlation correlations, i.e. $\Delta\text{O}_3/\Delta\text{CO} > 0$, indicate the formation of ozone. Negative correlations can (outside of stratospheric influence) indicate destruction of ozone or in-mixing of different air masses, which may also apply when a lack of correlation is observed (Parrish et al., 1993; Trainer et al., 2000; Voulgarakis et al., 2011, and references therein).

Figure 7 shows scatterplots of O_3 vs. CO during each of the four monsoon months with colour-coding indicating relative latitude. For all months, the slope $\Delta\text{O}_3/\Delta\text{CO}$ changes from positive at the southernmost latitudes to negative at First of all, the low latitude data ($-10^\circ < \Delta\text{lat} < -5^\circ$) combine low O_3 values (< 50 ppb) with about 75–100 ppb CO. With the exception of September (which has few statistically significant slopes at all in the low latitude band) the $\Delta\text{O}_3/\Delta\text{CO}$ slopes are significant and positive. At the northern edge of the UTAC ($\Delta\text{lat} \sim 15^\circ$). August is the month with the clearest latitudinal pattern in the slope $\Delta\text{O}_3/\Delta\text{CO}$: strong, positive relationships are observed in the south and immediately north of the transition point (0 again

with the exception of September, slopes are negative whereas August has positive values throughout except for $\Delta\text{lat} < 15^\circ$. The correlation slopes north of -5° vary considerably. Here O_3 values are definitely higher; they are however not well correlated with the generally similar CO values between 75 and about 110 (Δlat), and negative correlations are found in the far north. Patterns in other months show some characteristics of the relationships observed in August, for example, positive correlations in the south in June and July and negative correlations in the north in all months. These relationships provide an indication ppb. These relationships for the monsoon months indicate that ozone forming regimes dominate in the south and also immediately north of the transition point, while in the northern part of the UTAC there is no clear potential for ozone formation (see also Sect. S6 and Fig. S28). Ambiguous relationships near the transition point are most likely related to this region being most strongly and recently affected by continental emissions and/or air masses influenced by mixing during their transport, resulting in a broader range of air mass ages or sources. S25 which shows the values of the slope as a function of relative latitude). All these tendencies are determined from the slope of $\Delta\text{O}_3/\Delta\text{CO}$ over a few degrees latitude which agrees with the range of 200–500 km used in an earlier study by Zahn et al. (2002, their Fig. 10). The As expected, correlations for the individual flights (not shown) yield similar qualitative results as expected since the time between the individual flights through the monsoon in one month is short (12–36 h) compared to the transport time of the air inside the UTAC (many days).

15 3.1.3 Vertical profiles over Chennai

The majority of flight time through the UTAC was spent at cruise altitude in a narrow altitude range between 10.3 and 11.9 km (see Fig. S4), providing limited insight into the vertical distribution of trace species in the UTAC along the flight route. However, the descent into and take-off ascent from Chennai airport provide us with some information in the vertical in the southern part of the UTAC, as the aircraft passes between ~ 11 km and ground level over a relatively short distance (~ 200 – 250 km) in approximately 30 min (Fig. S4). During this time the aircraft moves from being within the UTAC into the free troposphere below and eventually into the boundary layer and vice versa. In situ data are available for most species down to ~ 2 km, with the exception of water vapour which is available down to ~ 5 km only, and NO_y , which is not available below ~ 10 km for these flights. Aerosol. Aerosol particle number concentrations during ascent are only available above 6 km because the CPCs need some time before they are ready to start the measurements. No whole air samples were collected on ascent and descent. Both ascent and descent took place during night, with landing times around 23:30 LT (local time) and take-off between 02:00 LT and 03:40 LT the following morning (Fig. S4). Descents into the airport were from a west–north–west direction towards the Bay of Bengal and final approaches from the east while the ascents were over land west of Chennai (except for the September flights which took off to the east). Similar flight times and patterns were followed for all flights except for July where when the approach into Chennai followed a route further north of Chennai before the final approach to the airport from the east (see Fig. S6).

While descending from cruise altitude, the aircraft moved from the westward flow of the UTAC into the eastward flow of the low level Somali Jet with its wind speed maximum around 850 hPa (Chakraborty et al., 2009). This is clearly visible in the wind direction measured-recorded by the CARIBIC aircraft shown in Fig. 8. In June and August this transition occurred between 6 and 7 km, while in September it was around 9 km altitude. In July, tropospheric wind speeds were much lower

than in the other months and there was no wind reversal evident from the measurements. This was a general feature of the meteorology on 15 and 16 July when the flights took place. Over a large region in Southeast India and out over the adjacent Bay of Bengal, wind speeds were very low from the surface up to 500 hPa (~5 km) which is about the height of the wind reversal seen in Fig. 8 in June and August. The corresponding ECMWF wind fields during the days of the flights are shown in Fig. S7 (745 hPa winds) and Fig. S8 (510 hPa winds). Over Central India and the Indian Ocean south of India there were eastward winds [in the lower troposphere](#) extending the Somali Jet over the Indian subcontinent and into the Bay of Bengal. But just around Chennai, winds were very calm. This has probably led to a trapping of the local pollution from the city of Chennai during these days in July 2008, whereas higher wind speeds in the lower troposphere were encountered in the other months.

Vertical trace gas and aerosol particle profiles during descent and ascent show a fairly consistent picture ~~during the monsoon season, with the exception of July (see, [although trace gas data for the two July flights \(see orange lines in Fig. 9\)](#)).~~ ~~Trace gas data for the two July flights~~ reflect the unique meteorological situation described above, particularly during the descent into Chennai, ~~which was very dry and had strongly enhanced O₃ (panel B) which, Very dry conditions (Fig. 9C) were measured while O₃ was strongly enhanced (Fig. 9B) and further~~ increased with decreasing altitude ~~and reached, reaching~~ 116 ppb at the lowermost point (not shown). These profiles were also characterised by high CO (~~panel Fig. 9A~~) between 6 and 9 km, which is above the level of wind direction change. There was no recognisable change in the number concentration of Aitken mode aerosol particles (~~panel Fig. 9D~~). In the free troposphere there was a weak north-westward flow (see Fig. 8) which would transport the pollution of Chennai and its ~~industrial sources industries~~ right to the region where the July flight descended into Chennai airport (see Fig. S6) while the other flights descended from the west–north-west, i.e. mostly upstream of the pollution sources in Chennai.

In the other months, ~~the~~ vertical “C”-shaped profiles of CO (see Fig. ~~9aA~~) reflect the position change outside and inside of the UTAC as the aircraft ascends into the upper troposphere. Moving upward from 2 km, mixing ratios of CO decrease until reaching the point where the wind direction changes, marking entry into the lower levels of the UTAC. Here, CO begins to increase, often reaching, and even exceeding, maxima observed at lower altitudes. The difference between maximum and minimum is most pronounced in June with mixing ratios in the middle troposphere being higher than in the other months, when mixing ratios are fairly similar. No significant differences between ascents and descents are observed. [The standard deviation calculated over moving 1.5 km altitude bins is shown as grey shading and supports the “C”-shaped profile.](#)

Profiles of O₃ (Fig. ~~9bB~~) show increasing mixing ratios with altitude, with no clear transition between free troposphere and UTAC and no significant differences between ascent and descent. A monthly trend is present, with the lowest values in August and the highest values in June, when the vertical gradient was also steepest. Monthly differences are most pronounced above 6 km. Conversely, water vapour (Fig. ~~9e, note logarithmic scale on x-axisC~~) decreased with altitude, with a similar vertical gradient during each month. June profiles were the driest, with the exception of the second flight into Chennai in September and the flight into Chennai in July (see above). June is at the beginning of the monsoon season in India when precipitation is not yet as ~~high strong~~ as during the ~~following monsoon subsequent~~ months.

Concentrations of the Aitken mode aerosol particles (N₁₂, Fig. ~~9d, logarithmic scale on x-axisD~~) show a positive vertical gradient, except for one descent in August which is variable with altitude but shows no consistent trend. There are no significant

monthly differences in concentration or gradient. Also N_{12} particle number concentrations during ascent and descent are more or less equal considering their general variability with altitude. This is expected since both descent and ~~take-off in Chennai occur many hours~~ ascent occur well after nightfall when all direct influence from the daytime convective activity has ceased. Part of the variability of the vertical N_{12} profiles is due to crossing of contrails of other ~~aircrafts~~ aircraft with locally very high aerosol particle number concentrations.

Measurements of O_3 profiles with MOZAIC (Measurement of OZone by Airbus In-service airCRAFT) aircraft over Chennai in 1996 and 1997 (Sahu et al., 2011) and Hyderabad in central India in 2006–2008 (Sahu et al., 2014) showed similar concentrations and a similar positive gradient with altitude. However, none of these observations documented a large increase towards the surface in the monsoon months as observed by CARIBIC in July 2008. MOZAIC CO profiles measured over Hyderabad in 2006–2008 (Sheel et al., 2014) were more or less constant at ~ 100 ppb throughout the free and upper troposphere and only showed an increase towards the surface below ~ 4 km. A pronounced increase of CO in the free troposphere as measured by CARIBIC in July 2008 has not been observed over Hyderabad in the summer months of these years. This corroborates that 15/16 July 2008 was an exceptional case with respect to the CO and O_3 profiles over Chennai.

3.2 Source regions of monsoon air

~~The focus of this study is on the export of polluted air masses from the UTAC, in other words how and where “leaks” from the UTAC occur and how this might influence long-distance pollution transport in the northern hemisphere. However, it is also of interest to investigate its~~ Before dealing with the fate of the air masses probed by CARIBIC (Sect. 3.3) we investigate the origin and subsequent processing of pollution during the trapping in the UTAC at low temperatures, pressures and water vapour under high insolation. In previous CARIBIC papers we have discussed the issue of the origin of certain pollutants (Schuck et al., 2010; Baker et al., 2011, 2012). Figure 10 shows trajectories calculated with the FLEXPART model for a representative case to identify the origin of the air that was sampled by the CARIBIC aircraft when flying through the UTAC. The backward trajectories for the ~~CARIBIC~~ flight to Chennai on 13 August 2008 are colour-coded with trajectory altitude ~~in kilometres~~ above sea-level (km a. s. l.). As the trajectory reliability decreases with time into the past (and future), we ~~used~~ use only the first 10 days for the source and receptor region analysis and in all subsequent plots.

For the northern ~~part~~ section of the flight track most of the observed air masses, approaching from the west, have resided for ~~many days~~ four days or longer inside the UTAC at altitudes (indicated by the trajectory colour in Fig. 10) at or above the CARIBIC flight altitude. ~~In the southern part~~ For the southern section, the air masses reached the CARIBIC flight track from the east after having been convected ~~from the lower troposphere into the upper troposphere~~ over or east of the Bay of Bengal, originally having followed an eastward flow in the lower troposphere with the Somali Jet over the Arabian Sea and Central and Southern India. Only when approaching Chennai airport at low altitudes we observed air coming directly from the west without having passed over the Bay of Bengal.

A summary of the source regions for ~~the air masses sampled by CARIBIC during the August 2008~~ all flights is shown in Fig. 11 ~~It shows by means of~~ where all points of the backward trajectories (starting at flight altitude) first descended below 5 km altitude. ~~The upper panel shows the source region distribution for the trajectories starting~~

north of, i.e. in the lower troposphere (left panels). The right panels show the corresponding 1- σ standard deviation of the percentages over the monsoon months June to September. The limit of 5 km was chosen because it is well below altitude of the wind reversal ; the lower panel shows the source region for CARIBIC observations in the southern part of the UTAC which separates the upper troposphere region with the monsoon UTAC from the lower troposphere (see also Fig. 8). Lower altitude thresholds (down to 1 km, not shown) do not change this picture significantly. This points to rapid more or less directly vertical convection from the lower troposphere into the UTAC region. For the northern part of the UTAC (upper left panel), the air came from Eastern India, the Indo-Gangetic-Plain as well as from the northern parts of the Bay of Bengal ; and Mainland Southeast Asia and the South China Sea. The air measured by CARIBIC in the southern part of the UTAC (lower left panel) originated in central and southern India, the western part of the Bay of Bengal and the western part of Mainland Southeast Asia. Apart from the contribution of Mainland Southeast Asia and the South China Sea, Arabian Sea off the western coast of India. The 1- σ standard deviations per grid box (right panels in Fig. 11) scale with the mean distribution, i.e. a high mean value is most often accompanied by a high standard deviation. This shows that the position of the source regions for the northern and southern part of the UTAC did not differ significantly. convective events is variable, i.e. a grid box with a high percentage in one month may have a lower mean percentage in the next month when the high percentage may be found in the neighbouring grid box. While the general pattern was similar for the other flights in June–August all flights in June–September 2008, the exact location of the convective uplift and hence the detailed pattern of the source regions varied and were more widely distributed than during August (see Figs. S29–S31 S26–S29).

3.3 Outflow from the UTAC

The following subsections describe the fate of the air and the contained trace species observed with CARIBIC after they have been processed in the monsoon UTAC. This includes to which regions they are transported to based on the FLEXPART trajectories and how long they have resided in the UTAC.

3.3.1 Receptor regions of monsoon air

FLEXPART forward trajectories were used to determine to where the air and the trace species, masses observed by CARIBIC at cruise altitude in the South Asian monsoon UTAC, were transported and by this revealing which regions were directly influenced by the outflow of the polluted air masses . We defined seven receptor regions, listed in Table 2: North America, Central Pacific, Central Africa and the Mediterranean over which we defined boxes reaching from the ground to the thermal tropopause. The trajectories are detected over these regions if they are within the defined boxes using the local thermal tropopause height output from the FLEXPART model along the trajectories. The South Asian monsoon region itself is defined as an ellipse with the centre at 80° E longitude while its latitude is between 22.7–27.9° N depending on the actual flight (see second to last column in Table 1). The monsoon centre latitude is determined from the zonal (west–east) wind reversal along the flight track using the wind speed and direction measured during flight recorded by the aircraft (see Sect. 3.1.1). To qualify as a monsoon trajectory, the trajectory has to stay for at least 70% of the 10 day period within the monsoon ellipse and below the thermal tropopause. Trajectories which stayed for at least 24 h above the thermal or dynamical tropopause ($PV > 2.5$ PVU)

were counted as TP (tropopause) or PV stratospheric trajectories, respectively. As expected, all but one of the trajectories which met the criterion for the dynamical tropopause also met the criterion for the thermal tropopause.

As each forward trajectory may cross several receptor regions, we determined the fraction of time the trajectory ~~stayed~~ spent inside each receptor region from the number of 30 min trajectory time-steps that were inside the receptor region. An example for this analysis is shown in Fig. 12 for the flight on 13 August ~~2008 where the flight track is shown by the thick red line.~~ 2008. Each panel shows all the forward trajectories (south of the northern cut-off) for this flight in grey. The trajectories which cross the different receptor regions are shown in red (North America), magenta (Central Pacific), green (Central Africa), blue (the Mediterranean), and orange (South Asian monsoon). The lowermost right panel shows the trajectories with stratospheric parts in yellow (for thermal tropopause criterion) and pink (dynamical tropopause criterion). As mentioned above, the dynamical tropopause usually is somewhat higher than the thermal tropopause. Therefore the pink trajectories form a subset of the yellow trajectories except for one trajectory which is classified as stratospheric according to the dynamical tropopause but not according to the thermal tropopause.

The aggregate results for the receptor region analysis ~~based on the forward trajectories~~ are shown in Fig. 13. It shows the percentages of trajectories reaching the seven receptor regions defined in Table 2 averaged for each month between June and September 2008. Since a trajectory may reach more than one receptor region (e.g. Central Africa and Mediterranean, Central Pacific and North America, or dynamical PV stratosphere and thermal TP stratosphere), the totals exceed 100 %. The least receptor region overlap is observed in September (~~the total is closest to 100%~~) while the trajectories in July reach the largest number of receptor regions. July is also different from the other months in that it has the largest fraction of outflow to the west, i.e. to Central Africa (green bar) and further on to the Mediterranean (blue bar). This may be a peculiarity ~~on~~ for 15/16 July 2008 when the flights took place. Note that in July there were only two flights and not four as in the other months.

The latitudinal distribution of the receptor regions (not shown) for the air sampled by the CARIBIC aircraft varies from flight to flight but the general tendency is that air sampled in the north is mostly either exported towards the east or entering the stratosphere while most air masses that are exported towards Africa and the Mediterranean have been sampled in the southern part of the flight track through the UTAC. ~~Interestingly~~ Importantly, air sampled in the middle of the UTAC, i.e. at the location of the wind reversal, and a few degrees south appears to have the highest likelihood of being transported to the stratosphere. In September, ~~the~~ transport is somewhat different, with less air sampled in the middle of the UTAC moving to the stratosphere but instead more air remains in the UTAC and the region where air is exported towards the east is expanding southwards. This shift in the latitudinal distribution may be the result of a weakening monsoon circulation towards the end of the monsoon season. The actual monsoon withdrawal as diagnosed by the India Meteorological Department however started in 2008 at the end of September ~~-(IMD, 2009)~~. One should also keep in mind that the monsoon contributes only partially to the air and the pollutants which reach the receptor regions. Especially for receptor regions far away, like e.g. North America, the monsoon will only have a limited influence. But in special cases the monsoon may even influence air mass composition as far away as the east coast of Canada (see Supplement Sect. S1 for a case documented by CARIBIC in September 2007).

3.3.2 Estimating transport times

An important cross-check of the FLEXPART trajectory calculations is possible by comparing with the photochemical age of air pollutants estimated from ratios of NMHCs measured in the whole air samples collected during the two flights in July and the first two flights in August 2008. ~~The photochemical age~~ Since sample collection only took place during the first two flight
5 per month, no samples are available for the last two flights in August. The samples from June and September did not give
consistent photochemical age estimates. The photochemical age is used as a proxy for the time elapsed since the pollutants
had been emitted into the air mass. Details of the NMHC age calculation have been published previously by Baker et al.
(2011). For air samples collected south of the wind reversal, that had recently convectively been lifted to cruise altitude, we
use an estimated mean OH concentration $\langle [\text{OH}] \rangle$ of 2.48×10^6 molecules cm^{-3} (Spivakovsky et al., 2000) ~~and emission ratios~~
10 ~~of 0.29 and 0.15 for propane/ethane and n-butane/ethane, respectively, were used. For air.~~ For samples collected north of
the wind reversal, ~~which had resided for a longer time inside the UTAC,~~ we instead applied an estimated $\langle [\text{OH}] \rangle$ of $1.44 \times$
 10^6 molecules cm^{-3} (Spivakovsky et al., 2000). Emission ratios of 0.29 and 0.15 for propane/ethane and n-butane/ethane,
respectively, were assumed. Figure 14 shows a clear clustering of the NMHC ages, with photochemically younger air in the
south ($\Delta\text{lat} < \sim 3^\circ$) which had recent contact with fresh emissions and older air in the north with more aged air having already
15 experienced several days of photochemical processing during transport in the UTAC. ~~For each air sample Fig. 14 shows the~~
~~mean photochemical age of the air sample together with the minimum and maximum age determined from the propane/ethane,~~
~~n-butane/ethane and n-butane/propane ratios~~ The NMHC based average ages in the two clusters are 4.5 days (south) compared
to 11 days (north).

The comparison of the mean chemical age of the air pollutants with the transport times estimated from the FLEXPART
20 trajectory calculations is shown in Fig. 15. ~~The~~ For July, the best fit was found when comparing the time since the air had last
been east of 90–95° E (~~Fig. 15 shows the time since the air was last east of.~~ For August, the correlations do not change
much for a source region between 85° E and 95° E. Table 3 lists the slopes and squared Pearson correlation coefficients R^2
for source regions at 80° E ~~).~~ to 100° E. For 95° E, the linear least-squares regression lines have slopes of 0.98–0.97 ± 0.19
and 0.93 ~~and ±0.20 and squared~~ and squared Pearson correlation coefficients R^2 of 0.87 and 0.68 for the flights in July and August, respec-
25 tively. Considering that the NMHC age ~~uses estimates use~~ uses estimates use surface emission ratios ~~estimated from based on~~ estimated from based on
ground-based data as the starting point for the age calculations and that convection (which is partly parameterised in the FLEXPART model)
is most frequent over the Bay of Bengal, a source region east of 90–95° E seems reasonable and fits to the source regions
discussed in Sect. 3.2. ~~Approximate~~ Although the degree of significance of the correlations is largely due to the existence of
two clusters of data, the approximate overall agreement between the two methods provides confidence that our interpretation
30 of pollutant distributions and transport within the UTAC is realistic. In most cases where there is a large disagreement between
NMHC chemical age and FLEXPART transport age, the NMHC ages show a large spread. Reasons for this may be mixing
with background air ~~containing NMHCs~~, different source ratios than assumed in the analysis or situations where the OH con-
centrations deviated from the assumed climatological averages used in the NMHC age calculations. Uncertainties ~~of in~~ of in $\langle [\text{OH}] \rangle$
of $\pm 25\%$ correspond to uncertainties of the derived NMHC ages of 20–33% (see Baker et al., 2011).

3.3.3 Monsoon UTAC “leak” rates

The South Asian summer monsoon UTAC is often described as a processing reactor for the pollution emitted at the surface which is rapidly transported upward by convection ~~and then to become~~ trapped in the UTAC (e.g. Park et al., 2008; Schuck et al., 2010; Randel and Jensen, 2013; Barret et al., 2016, and references therein). However, the horizontal wind fields shown in Fig. 1 and the forward trajectories in Fig. 12 indicate that the trapping is temporary ~~-, i.e. the trajectories do not stay in the monsoon UTAC forever. Already 10 days after the flight, around 50 % of the trajectories have left the UTAC (see Fig. 16 described below).~~ At the south-western part of the UTAC, ~~some~~ air escapes to Central Africa, part of which may return via the Mediterranean and the Middle East to become again entrained in the UTAC in the northwest. In the northeastern region, air is leaving the UTAC with the eastward jet stream and is transported over China towards the Pacific and finally Northern America.

Quantifying ~~this loss these losses~~ is the goal of the leak rate analysis described below.

The calculated trajectories have been used to estimate the residence time of the observed air inside the monsoon ellipse defined above. For this analysis, only the trajectories along the flight track that ~~start~~started inside the ellipse are used. The number of trajectories remaining within the ellipse was determined for the preceding and following 10 days at time steps of 6 h centred around the middle of the time period the flight track spent inside the ellipse, i.e. the middle from the aircraft entering the ellipse at its northern edge and the touch-down at Chennai and vice versa for southward and northbound flights, respectively.

This analysis is similar to ~~leak rates calculated~~the leak rate calculations by Randel and Park (2006, their Fig. 14).

The results, colour-coded for flight month, are shown in Fig. 16. The solid coloured lines show the monthly means while the dashed black line indicates the average over all months. On average, 65 % of the trajectories had resided inside the monsoon ellipse for at least 10 days while 30 % of the air ~~was had become~~ entrained within the last three days prior to ~~the measurements~~measurement. Following the air masses after ~~the their~~ measurement shows a different picture: after 6 days only 50 % of the trajectories, on average, ~~are still had remained~~ within the ellipse. However, while fewer trajectories were within the ellipse before the measurement in August, they tended to remain inside longer after the measurement than in the other months. Especially in June and September, the exit from the ellipse was more rapid than in July and August, related to the weaker monsoon circulation during these months. The calculated leak rates are higher, i.e. the trajectories leave the ~~trajectory~~UTAC region faster, than those calculated by (Randel and Park, 2006) which is consistent with the much larger monsoon anticyclone area definition used by these authors.

An explanation for the asymmetric shape of the calculated leak rates ~~could be is~~ related to the position of the aircraft within the UTAC and hence within the monsoon ellipse defined above. The flight tracks cross the western part of the ellipse. The UTAC has two main points of air discharge: one in the south-west where air is transported westwards towards Africa and one in the north-east where it is transported eastwards towards China and the Pacific Ocean. In the northern part of our flight track inside the UTAC, the air masses observed had not left towards Africa but stayed inside the UTAC. In the forward direction, the air masses have a chance of leaving the UTAC at its north-eastern part, i.e. towards China and the Pacific Ocean. Having traversed to the southern part, the air masses observed have not left towards the Pacific but stayed inside the UTAC. But looking forward again, the air masses have a chance of leaving the UTAC towards Africa. Since the calculated leak rates are an average

over all trajectories started inside the UTAC, the tendency that the air masses have already been for quite some time inside the UTAC (at least the majority of the trajectories) while looking forwards, the air masses have a higher chance of leaving the UTAC quickly (or at least faster than they have entered the UTAC) seems to be consistent with our understanding of the monsoon circulation. In August, which from all CARIBIC data seems to be the most representative monsoon month (red lines in Fig. 16), the UTAC contains the air masses more strongly than in the other months. In addition, Figs. ~~S32 and S33~~ S30 and S31 show that the trapping efficiency ~~is comparable~~ changes little even when considering altitudes ~~that are~~ 2 km above the actual ~~flight altitudes~~ flight-level. This is somewhat unexpected. As the UTAC has its maximum some kilometres above the actual flight altitude of the CARIBIC aircraft of $\sim 11\text{--}12$ km (Park et al., 2008), ~~an even a~~ stronger confinement at altitudes above the CARIBIC flight altitudes ~~would be~~ is expected.

10 4 Conclusions

The data from the CARIBIC passenger aircraft observatory discussed in this study cover the South Asian summer monsoon season 2008 from June to September. ~~The flights largely~~ Even though the flights crossed the western part of the ~~summer monsoon UTAC at an~~ monsoon UTAC and not its centre and the cruise altitude of ~ 11 km ~~which is believed to be at its bottom part where pollution levels are possibly lower than a few kilometres aloft where the UTAC is even stronger~~ is at the lower boundary of the UTAC (e.g. Park et al., 2008). ~~Figure 7, however, showing tracer-tracer, Figs. 6 and 7 show systematic profiles and trace gas~~ correlations over a distance of 3500 km (approximately from Teheran, Iran to Chennai, India), ~~demonstrates the extent of the UTAC and the remarkable consistency of the CARIBIC observations, where trace gas distributions show regular patterns during monthly flights and even from month to month~~ as previously reported by Schuck et al. (2010) and ~~Baker et al., 2011~~ Earlier Baker et al. (2011). ~~This matches earlier observations from CARIBIC phase 1 during flights from Germany to Colombo, Sri Lanka and Male, Maldives (not shown)~~ This matches earlier observations from CARIBIC phase 1 during flights from Germany to Colombo, Sri Lanka and Male, Maldives (not shown) in the summers 1998–2000, despite consisting of a more limited chemical dataset (Hermann et al. (2003); Zahn et al. (2002) and unpublished data), ~~also consistently show a similar development of the monsoon in terms of trace gas and aerosol particle distributions during flights from Germany to Colombo, Sri Lanka and Male, Maldives (not shown). These results will be published separately but underscore that the present dataset is representative even though it consists of a few flights per month only.~~

25 In accordance with our current understanding of the South Asian summer monsoon and in particular its role trapping surface air that was rapidly transported upwards by convective activity, all the CARIBIC observations during the monsoon months in this region, although they were made in different years, fit the same overall picture of pollution build-up in the UTAC. Starting from this consistent dataset, of particular interest is on the one hand the understanding of the chemical composition of the air in the UTAC and on the other hand the export of this air to other regions, for which the CARIBIC flight to Toronto in September 30 2007 (see Sect. S1) gives a good example.

Based on the measured reversal of the zonal wind at flight altitude across the centre of the UTAC located at 27° N in June to 23° N in September (Table 1, cf. New Delhi 28.4° N, Calcutta 22.3° N), the chemical and aerosol particle data are presented using relative latitude with respect to the wind reversal and by doing so provide a very consistent picture of humid, recently

polluted, low O₃, medium CO air and low NO_y air with a high burden of aerosol particles in the south and a strengthening tendency (increasing CO and O₃, declining humidity) towards the centre of the UTAC. Northwards from there dry air, with higher NO_y, but strongly declining CO, moderately declining O₃ (up to a relative latitude Δlat of around 12°) and low aerosol particle number concentrations is observed.

5 The vertical profiles of O₃ and CO over Chennai are very distinct compared to other profile observations over India (cf. Sheel et al. (2014); Sahu et al. 2014). They are likely influenced by the local emissions in the Chennai area together with the advection of clean maritime air and polluted air from other parts of India and the surrounding region to form the characteristic “C”-shape observed for CO in all months except July. In that month a strong free tropospheric CO enhancement of up to 116 ppb was observed which cannot be explained solely by local convection of polluted surface air but is instead probably due to long-range
10 transport of polluted air masses. Detailed modelling studies [with the WRFChem online regional chemistry transport model](#) to understand these vertical profiles ~~are currently ongoing and will be~~ [have been](#) published separately (Ojha et al., 2015).

Hydrocarbon ratios used in photochemical age of air calculations show that the air masses in the southern part of the UTAC are younger (chemical ages between 3.5 and 6.5 days) than in the north (chemical ages between 10 and 13.5 days). The clustering of the chemical ages compares well with that based on the transport age determined from the FLEXPART
15 backward trajectories, namely 1–7 days compared to 7–14 days for transport from 95° E to the CARIBIC flight track. The spread in the FLEXPART transport ages is larger and they are in general higher by 0.5–1.5 days. Given the uncertainties of air mass trajectory calculations, the problems in how to determine its starting point in time over polluting sources and given the uncertainty in photochemical age that may be affected by dilution with background air, the correspondence is encouraging.

Air sampled by CARIBIC originated from a large region. Although the convection over the Bay of Bengal is greatest, for a
20 quantification of its effect on pollution the vertical transport has to be combined with the emission source distributions which is beyond this study-. [For the vertical profiles such a study has been done by](#) Ojha et al. (2015). Instead we have focused on the FLEXPART backward trajectory based footprint (air at cruise level that had come from below 5 km) for air in the southern and northern part of the UTAC. For the southern part, the footprint is situated somewhat more to the [south and west](#). For August the surface area of the footprint is largest (~~Fig. 14~~ [see Figs. S26–S29](#)). When the UTAC wanes in September, and
25 its centre moves south to reach 23° N north, the footprint likewise shifts southward [and is more concentrated over the Indian subcontinent than in the other months](#). However, no major differences in footprint for air in the southern compared to the northern part of the UTAC exists; the age difference seems to be the fundamental difference. [In other words, the difference between the two regimes is due to the time elapsed since fresh pollution was injected into the UTAC.](#)

The receptor region analyses and the “leak” rates show that air in the southern part of the UTAC is mostly in an ozone
30 forming chemical regime (Fig. 7) and part of it is exported towards Central Africa and the Mediterranean. In contrast, the air in the northern part, which features an ozone neutral or partially even ozone destroying chemical regime, is exported towards China and the Pacific ocean and in rare cases even up to the east coast of North America (Sect. S1). Export from the UTAC into the stratosphere peaked in June and July (Fig. 13). With CO values declining from June onward, this implies an “optimal” input of CO into the lowermost stratosphere. However, ~~around~~ [approximately](#) two thirds of the air is dispersed
35 within the troposphere. Such transport to the stratosphere has been observed in a similar way by the German HALO (High

Altitude and Long range) research aircraft, which detected monsoon pollution transported to the lowermost stratosphere over Europe in late summer 2012 during the TACTS (Transport And Composition in the upper troposphere/lowermost stratosphere) campaign (Roiger, 2014).

The large scale movement in the UTAC as in a large scale atmospheric “merry-go-around” is not without losses (Fig. 16).
5 While surface air very high in pollutants reaches the UTAC from below and becomes trapped, similar amounts of air leak out of the system, mostly at its northeastern and southwestern edges. Still the trapping process is impressive. Even going back in time 10 days prior to sampling by CARIBIC, on average 65 % of the back trajectories had resided within the UTAC defined for this calculation as an ellipse. After having been probed by CARIBIC, only 40 % of the trajectories stay in the UTAC ellipse for more than 10 days. This asymmetry is an artifact of the geographical skew in the sampling by CARIBIC. Interestingly,
10 calculations show that the leakage rates 2 km above cruise altitude of CARIBIC are not significantly lower (Sect. S8). A mass balance of the UTAC is beyond the scope of this work. No doubt, also air from outside the UTAC is being entrained, leading to dilution that intensifies towards its borders.

~~In-The population of~~ the monsoon source region of South Asia ~~lived-was~~ about 1.4 billion people in 2008 (~~linearly interpolated to the year 2008 from data for 2000 and estimates for 2010~~) ~~and~~ and the population is still growing. Together
15 with the economic development in this region, this means that the pollutant emissions today are larger than in 2008 and will further increase in the future. This also encompasses export of even more polluted air as shown in this study with implications for the atmospheric chemistry and air quality in the receiving regions.

The Supplement related to this article is available online at doi:10.5194/acp-0-1-2016-supplement.

Acknowledgements. We wish to thank all CARIBIC partners as well as Lufthansa, especially T. Dauer and A. Waibel, and Lufthansa
20 Technik for their ongoing support for many years. We especially acknowledge D. Scharffe, C. Koepfel and S. Weber for the operation of this complex platform. The FLEXPART model ~~has-been-was~~ provided by A. Stohl at the Norwegian Institute for Air Research (NILU) and was used with meteorological data from the European Centre for Medium-Range Weather Forecasts (ECMWF).

The article processing charges for this open-access publication
25 have been covered by the Max Planck Society.

References

- Assonov, S. S., Brenninkmeijer, C. A. M., Schuck, T. J., and Taylor, P.: Analysis of ^{13}C and ^{18}O isotope data of CO_2 in CARIBIC aircraft samples as tracers of upper troposphere/lower stratosphere mixing and the global carbon cycle, *Atmos. Chem. Phys.*, 10, 8575–8599, doi:10.5194/acp-10-8575-2010, 2010.
- 5 Baker, A. K., Slemr, F., and Brenninkmeijer, C. A. M.: Analysis of non-methane hydrocarbons in air samples collected aboard the CARIBIC passenger aircraft, *Atmos. Meas. Tech.*, 3, 311–321, doi:10.5194/amt-3-311-2010, 2010.
- Baker, A. K., Schuck, T. J., Slemr, F., van Velthoven, P., Zahn, A., and Brenninkmeijer, C. A. M.: Characterization of non-methane hydrocarbons in Asian summer monsoon outflow observed by the CARIBIC aircraft, *Atmos. Chem. Phys.*, 11, 503–518, doi:10.5194/acp-11-503-2011, 2011.
- 10 Baker, A. K., Schuck, T. J., Brenninkmeijer, C. A. M., Rauthe-Schöch, A., Slemr, F., van Velthoven, P. F. J., and Lelieveld, J.: Estimating the contribution of monsoon-related biogenic production to methane emissions from South Asia using CARIBIC observations, *Geophys. Res. Lett.*, 10, L10813, doi:10.1029/2012GL051756, 2012.
- [Barret, B., Sauvage, B., Bennouna, Y., and Le Flochmoen, E.: Upper tropospheric CO and O₃ budget during the Asian Summer Monsoon. *Atmos. Chem. Phys. Discuss.*, doi:10.5194/acp-2015-1011, 2016.](#)
- 15 Brenninkmeijer, C. A. M., Crutzen, P., Boumard, F., Dauer, T., Dix, B., Ebinghaus, R., Filippi, D., Fischer, H., Franke, H., Frieß, U., Heintzenberg, J., Helleis, F., Hermann, M., Kock, H. H., Koepfel, C., Lelieveld, J., Leuenberger, M., Martinsson, B. G., Miemczyk, S., Moret, H. P., Nguyen, H. N., Nyfeler, P., Oram, D., O’Sullivan, D., Penkett, S., Platt, U., Pupek, M., Ramonet, M., Randa, B., Reichelt, M., Rhee, T. S., Rohwer, J., Rosenfeld, K., Scharffe, D., Schlager, H., Schumann, U., Slemr, F., Sprung, D., Stock, P., Thaler, R., Valentino, F., van Velthoven, P., Waibel, A., Wandel, A., Waschitschek, K., Wiedensohler, A., Xueref-Remy, I., Zahn, A., Zech, U., and Ziereis, H.: Civil aircraft for the regular investigation of the atmosphere based on an instrumented container: The new CARIBIC system, *Atmos. Chem. Phys.*, 7, 4953–4976, doi:10.5194/acp-7-4953-2007, 2007.
- 20 Brough, N., Reeves, C. E., Penkett, S. A., Stewart, D. J., Dewey, K., Kent, J., Barjat, H., Monks, P. S., Ziereis, H., Stock, P., Huntrieser, H., and Schlager, H.: Intercomparison of aircraft instruments on board the C-130 and Falcon 20 over southern Germany during EXPORT 2000, *Atmos. Chem. Phys.*, 3, 2127–2138, doi:10.5194/acp-3-2127-2003, 2003.
- 25 ~~Center for International Earth Science Information Network (CIESIN)/Columbia University: National aggregates of geospatial data collection: Population, Landscape, And Climate Estimates, Version 3 (PLACE III), NASA Socioeconomic Data and Applications Center (SEDAC), Palisades, NY, USA, available online at: <http://sedac.ciesin.columbia.edu/data/set/nagde-population-landscape-climate-estimates-v3>, last access: 6 February 2015, 2012.~~
- [Chakraborty, A., Nanjundiah, R. S., and Srinivasan, J.: Impact of African orography and the Indian summer monsoon on the low-level Somali jet, *Int. J. Climatol.*, 29, 983–992, doi:10.1002/joc.1720, 2009.](#)
- 30 Chen, B., Xu, X. D., Yang, S., and Zhao, T. L.: Climatological perspectives of air transport from atmospheric boundary layer to tropopause layer over Asian monsoon regions during boreal summer inferred from Lagrangian approach, *Atmos. Chem. Phys.*, 12, 5827–5839, doi:10.5194/acp-12-5827-2012, 2012.
- Crawford, J. and Pan, L.: Atmospheric composition and the Asian monsoon: Results from a side meeting at the 12th IGAC Science Conference in Beijing, 17–21 September 2012, *SPARC Newsletter*, 40, 67, 2013.
- Devasthale, A. and Fueglistaler, S.: A climatological perspective of deep convection penetrating the TTL during the Indian summer monsoon from the AVHRR and MODIS instruments, *Atmos. Chem. Phys.*, 10, 4573–4582, doi:10.5194/acp-10-4573-2010, 2010.

- Dyroff, C., Zahn, A., Christner, E., Forbes, R., Tompkins, A. M., and van Velthoven, P. F. J.: Comparison of ECMWF analysis and forecast humidity data to CARIBIC upper troposphere and lower stratosphere observations, *Quart. J. Roy. Meteorol. Soc.*, doi:10.1002/qj.2400, ~~2014~~, published online-141, 833–844, doi:10.1002/qj.2400, 2015.
- Fairlie, T. D., Vernier, J.-P., Natarajan, M., and Bedka, K. M.: Dispersion of the Nabro volcanic plume and its relation to the Asian summer monsoon, *Atmos. Chem. Phys.*, 14, 7045–7057, doi:10.5194/acp-14-7045-2014, 2014.
- Fishman, J. and Crutzen, P. J.: The origin of ozone in the troposphere, *Nature*, 274, 855–858, doi:10.1038/274855a0, 1978.
- Garny, H. and Randel, W. J.: Dynamic variability of the Asian monsoon anticyclone observed in potential vorticity and correlations with tracer distributions, *J. Geophys. Res.*, 118, 13421–13433, doi:10.1002/2013JD020908, 2013.
- Hermann, M. and Wiedensohler, A.: Counting efficiency of condensation particle counters at low-pressures with illustrative data from the upper troposphere, *J. Aerosol Sci.*, 32, 975–991, doi:10.1016/S0021-8502(01)00037-4, 2001.
- Hermann, M., Heintzenberg, J., Wiedensohler, A., Zahn, A., Heinrich, G., and Brenninkmeijer, C. A. M.: Meridional distributions of aerosol particle number concentrations in the upper troposphere and lower stratosphere obtained by Civil Aircraft for Regular Investigation of the Atmosphere Based on an Instrument Container (CARIBIC) flights, *J. Geophys. Res.*, 108, 4114, doi:10.1029/2001JD001077, 2003.
- IMD: —India Meteorological Department (~~IMD~~)~~Monsoon~~—~~website~~Annual Report 2008, available at: http://www.imd.gov.in/section/nhae/dynamic/Monsoon_frame.htm <http://metnet.imd.gov.in/indnews/ar2008.pdf>, last access: 619 February 2015, 2014–2016, 2009.
- Kar, J., Bremer, H., Drummond, J. R., Rochon, Y. J., Jones, D. B. A., Nichitui, F., Zou, J., Liu, J., Gille, J. C., Edwards, D. P., Deeter, M. N., Francis, G., Ziskin, D., and Warner, J.: Evidence of vertical transport of carbon monoxide from Measurements of Pollution in the Troposphere (MOPITT), *Geophys. Res. Lett.*, 31, L23105, doi:10.1029/2004GL021128, 2004.
- Kurokawa, J., Ohara, T., Morikawa, T., Hanayama, S., Janssens-Maenhout, G., Fukui, T., Kawashima, K., and Akimoto, H.: Emissions of air pollutants and greenhouse gases over Asian regions during 2000–2008: Regional Emission inventory in ASia (REAS) version 2, *Atmos. Chem. Phys.*, 13, 11 019–11058, doi:10.5194/acp-13-11019-2013, 2013.
- Lawrence, M. G. and Lelieveld, J.: Atmospheric pollutant outflow from southern Asia: a review, *Atmos. Chem. Phys.*, 10, 11017–11096, doi:10.5194/acp-10-11017-2010, 2010.
- Lelieveld, J., Berresheim, H., Borrmann, S., Crutzen, P. J., Dentener, F. J., Fischer, H., Feichter, J., Flatau, P. J., Heland, J., Holzinger, R., Korrmann, R., Lawrence, M. G., Levin, Z., Markowicz, K. M., Mihalopoulos, N., Minikin, A., Ramanathan, V., de Reus, M., Roelofs, G. J., Scheeren, H. A., Sciare, J., Schlager, H., Schultz, M., Siegmund, P., Steil, B., Stephanou, E. G., Stier, P., Traub, M., Warneke, C., Williams, J., and Ziereis, H.: Global air pollution crossroads over the Mediterranean, *Science*, 298, 794–799, doi:10.1126/science.1075457, 2002.
- Lelieveld, J., Brühl, C., Jöckel, P., Steil, B., Crutzen, P. J., Fischer, H., Giorgetta, M. A., Hoor, P., Lawrence, M. G., Sausen, R., and Tost, H.: Stratospheric dryness: model simulations and satellite observations, *Atmos. Chem. Phys.*, 7, 1313–1332, doi:10.5194/acp-7-1313-2007, 2007.
- Li, Q., Jacob, D. J., Logan, J. A., Bey, I., Yantosca, R. M., Liu, H., Martin, R. V., Fiore, A. M., Field, B. D., Duncan, B. N., and Thouret, V.: A tropospheric ozone maximum over the Middle East, *Geophys. Res. Lett.*, 28, 3235–3238, doi:10.1029/2001GL013134, 2001.
- Liang, Q., Jaeglé, L., Hudman, R. C., Turquety, S., Jacob, D. J., Avery, M. A., Browell, E. V., Sachse, G. W., Blake, D. R., Brune, W., Ren, X., Cohen, R. C., Dibb, J. E., Fried, A., Fuelberg, H., Porter, M., Heikes, B. G., Huey, G., Singh, H. B., and Wennberg, P. O.: Summertime influence of Asian pollution in the free troposphere over North America, *J. Geophys. Res.*, 112, D12S11, doi:10.1029/2006JD007919, 2007.

- Liu, H., Jacob, D. J., Bey, I., Yantosca, R., Duncan, B. N., and Sachse, G. W.: Transport pathways for Asian pollution outflow over the Pacific: interannual and seasonal variations, *J. Geophys. Res.*, 108, 8786, doi:10.1029/2002JD003102, 2003.
- Liu, J. J., Jones, D. B. A., Worden, J. R., Noone, D., Parrington, M., and Kar, J.: Analysis of the summertime buildup of tropospheric ozone abundances over the Middle East and North Africa as observed by the Tropospheric Emission Spectrometer instrument, *J. Geophys. Res.*, 114, D05304, doi:10.1029/2008JD010993, 2009.
- Ojha, N., Pozzer, A., Rauthe-Schöch, A., Baker, A. K., Yoon, J., Brenninkmeijer, C. A. M., and Lelieveld, J.: ~~WRF-Chem simulations of ozone and CO~~ Ozone and carbon monoxide over India during the summer monsoon: Regional emissions and transport, *Atmos. Chem. Phys. Discuss.*, ~~submitted~~, 15, 21133–21176, doi:10.5194/acpd-15-21133-2015, resubmitted, 2015.
- O'Sullivan, D. A.: Temporal and spatial variability of halogenated compounds and other trace gases, Ph.D. thesis, University of East Anglia, Norwich, United Kingdom, 2007.
- Pan, L., Crawford, J., Tanimoto, H., Lawrence, M., Panday, A., Babu, S. S., Barret, B., Schlager, H., Konopka, P., and Bian, J.: Report on the Atmospheric Composition and the summer Asian Monsoon (ACAM) workshop, 9–12 June 2013, Kathmandu, Nepal, SPARC Newsletter, 42, 40–45, 2014.
- Park, M., Randel, W. J., Emmons, L. K., Bernath, P. F., Walker, K. A., and Boone, C. D.: Chemical isolation in the Asian monsoon anticyclone observed in Atmospheric Chemistry Experiment (ACE-FTS) data, *Atmos. Chem. Phys.*, 8, 757–764, doi:10.5194/acp-8-757-2008, 2008.
- Parrish, D. D., Holloway, J. S., Trainer, M., Murphy, P. C., Fehsenfeld, F. C., and Forbes, G. L.: Export of North American ozone pollution to the North Atlantic ocean, *Science*, 259, 1436–1439, doi:10.1126/science.259.5100.1436, 1993.
- Parrish, D. D., Trainer, M., Holloway, J. S., Yee, J. E., Warshawsky, M. S., Fehsenfeld, F. C., Forbes, G. L., and Moody, J. L.: Relationships between ozone and carbon monoxide at surface sites in the North Atlantic region, *J. Geophys. Res.*, 103, 13357–13376, doi:10.1029/98JD00376, 1998.
- Patra, P. K., Niwa, Y., Schuck, T. J., Brenninkmeijer, C. A. M., Machida, T., Matsueda, H., and Sawa, Y.: Carbon balance of South Asia constrained by passenger aircraft CO₂ measurements, *Atmos. Chem. Phys.*, 11, 4163–4175, doi:10.5194/acp-11-4163-2011, 2011.
- Randel, W. J. and Jensen, E. J.: Physical processes in the tropical tropopause layer and their roles in a changing climate, *Nature Geosci.*, 6, 169–176, doi:10.1038/ngeo1733, 2013.
- Randel, W. J. and Park, M.: Deep convective influence on the Asian summer monsoon anticyclone and associated tracer variability observed with Atmospheric Infrared Sounder (AIRS), *J. Geophys. Res.*, 111, D12314, doi:10.1029/2005JD006490, 2006.
- Randel, W. J., Park, M., Emmons, L., Kinnison, D., Bernath, P., Walker, K. A., Boone, C., and Pumphrey, H.: Asian monsoon transport of pollution to the stratosphere, *Science*, 328, 611–613, doi:10.1126/science.1182274, 2010.
- Roiger, A.: private communication, 2014.
- Sahu, L. K., Lal, S., Thouret, V., and Smit, H. G.: Climatology of tropospheric ozone and water vapour over Chennai: a study based on MOZAIC measurements over India, *Int. J. Climatol.*, 31, 920–936, doi:10.1002/joc.2128, 2011.
- Sahu, L. K., Sheel, V., Kajino, M., Deushi, M., Gunthe, S. S., Sinha, P. R., Sauvage, B., Thouret, V., and Smit, H. G.: Seasonal and interannual variability of tropospheric ozone over an urban site in India: a study based on MOZAIC and CCM vertical profiles over Hyderabad, *J. Geophys. Res.*, 119, 3615–3641, doi:10.1002/2013JD021215, 2014.
- Scharffe, D., Slemr, F., Brenninkmeier, C. A. M., and Zahn, A.: Carbon monoxide measurements onboard the CARIBIC passenger aircraft using UV resonance fluorescence, *Atmos. Meas. Tech.*, 5, 1753–1760, doi:10.5194/amt-5-1753-2012, 2012.

- Scheeren, H. A., Lelieveld, J., Roelofs, G. J., Williams, J., Fischer, H., de Reus, M., de Gouw, J. A., C. Warneke, Holzinger, R., Schlager, H., Klüpfel, T., Bolder, M., van der Veen, C., and Lawrence, M.: The impact of monsoon outflow from India and Southeast Asia in the upper troposphere over the eastern Mediterranean, *Atmos. Chem. Phys.*, 3, 1589–1608, doi:10.5194/acp-3-1589-2003, 2003.
- Schuck, T. J., Brenninkmeijer, C. A. M., Slemr, F., Xueref-Remy, I., and Zahn, A.: Greenhouse gas analysis of air samples collected onboard the CARIBIC passenger aircraft, *Atmos. Meas. Tech.*, 2, 449–464, doi:10.5194/amt-2-449-2009, 2009.
- Schuck, T. J., Brenninkmeijer, C. A. M., Baker, A. K., Slemr, F., van Velthoven, P. F. J., and Zahn, A.: Greenhouse gas relationships in the Indian summer monsoon plume measured by the CARIBIC passenger aircraft, *Atmos. Chem. Phys.*, 10, 3965–3984, doi:10.5194/acp-10-3965-2010, 2010.
- Sheel, V., Sahu, L. K., Kajino, M., Deushi, M., Stein, O., and Nedelec, P.: Seasonal and interannual variability of carbon monoxide based on MOZAIC observations, MACC reanalysis, and model simulations over an urban site in India, *J. Geophys. Res.*, 119, 9123–9141, doi:10.1002/2013JD021425, 2014.
- Spivakovsky, C. M., Logan, J. A., Montzka, S. A., Balkanski, Y. J., Foreman-Fowler, M., Jones, D. B. A., Horowitz, L. W., Fusco, A. C., Brenninkmeijer, C. A. M., Prather, M. J., Wofsy, S. C., and McElroy, M. B.: Three-dimensional climatological distribution of tropospheric OH: update and evaluation, *J. Geophys. Res.*, 105, 8931–8980, doi:10.1029/1999JD901006, 2000.
- Stohl, A., Forster, C., Frank, A., Seibert, P., and Wotawa, G.: Technical note: The Lagrangian particle dispersion model FLEXPART version 6.2, *Atmos. Chem. Phys.*, 5, 2461–2474, doi:10.5194/acp-5-2461-2005, 2005.
- Stohl, A., Sodemann, H., Eckhardt, S., Frank, A., Seibert, P., and Wotawa, G.: The Lagrangian particle dispersion model FLEXPART version 8.2, Tech. rep., Norwegian Institute of Air Research (NILU), Kjeller, Norway, available at: <http://flexpart.eu/>, last access: 6¹⁹ February 2015, 2016, 2010.
- Trainer, M., Parrish, D. D., Goldan, P. D., Roberts, J., and Fehsenfeld, F. C.: Review of observation-based analysis of the regional factors influencing ozone concentrations, *Atmos. Environ.*, 34, 2045–2061, doi:10.1016/S1352-2310(99)00459-8, 2000.
- Traub, M. and Lelieveld, J.: Cross-tropopause transport over the eastern Mediterranean, *J. Geophys. Res.*, 108, 4712, doi:10.1029/2003JD003754, 2003.
- Umezawa, T., Baker, A. K., Oram, D., Sauvage, C., O’Sullivan, D., Rauthe-Schöch, A., Montzka, S. A., Zahn, A., and Brenninkmeijer, C. A. M.: Methyl chloride in the upper troposphere observed by the CARIBIC passenger aircraft observatory: large-scale distributions and Asian summer monsoon outflow, *J. Geophys. Res.*, 119, 5542–5558, doi:10.1002/2013JD021396, 2014.
- [Umezawa, T., Baker, A. K., Brenninkmeijer, C. A. M., Zahn, A., Oram, D. E., and van Velthoven, P. F. J.: Methyl chloride as a tracer of tropical tropospheric air in the lowermost stratosphere inferred from IAGOS-CARIBIC passenger aircraft measurements, *J. Geophys. Res.*, 120, 12 313–12 326, doi:10.1002/2015JD023729, 2015.](#)
- [Vogel, B., Günther, G., Müller, R., Groß, J.-U., and Riese, M.: Impact of different Asian source regions on the composition of the Asian monsoon anticyclone and of the extratropical lowermost stratosphere, *Atmos. Chem. Phys.*, 15, 13699–13716, doi:10.5194/acp-15-13699-2015, 2015.](#)
- Voulgarakis, A., Telford, P. J., Aghedo, A. M., Braesicke, P., Faluvegi, G., Abraham, N. L., Bowman, K. W., Pyle, J. A., and Shindell, D. T.: Global multi-year O₃-CO correlation patterns from models and TES satellite observations, *Atmos. Chem. Phys.*, 11, 5819–5838, doi:10.5194/acp-11-5819-2011, 2011.
- Weigelt, A., Hermann, M., van Velthoven, P. F. J., Brenninkmeijer, C. A. M., Schlaf, G., Zahn, A., and Wiedensohler, A.: Influence of clouds on aerosol particle number concentrations in the upper troposphere, *J. Geophys. Res.*, 114, D01204, doi:10.1029/2008JD009805, 2009.

Table 1. CARIBIC2 flights to Chennai/India in 2008. Listed are the flight number, date of departure and flight direction. Column 4 gives the northern cut-off for the trajectory analysis which was selected for each month to exclude trajectories belonging to the eastward jet stream. ~~The last column~~ Column 5 lists the latitude of the wind reversal along each flight track which is used as indicator of centre latitude of the monsoon UTAC at flight altitude (see Fig. 4). The last column indicates whether air samples have been collected or not.

Flight no.	Direction	Date of departure	Northern cut-off	Monsoon centre latitude	<u>Air samples ?</u>
236	southward	18 June 2008	36.5° N	27.9° N	<u>yes</u>
237	northward	18 June 2008	36.5° N	25.5° N	<u>yes</u>
238	southward	19 June 2008	36.5° N	25.8° N	<u>no</u>
239	northward	19 June 2008	36.5° N	24.4° N	<u>no</u>
240	southward	15 July 2008	40.0° N	26.7° N	<u>yes</u>
241	northward	15 July 2008	40.0° N	26.1° N	<u>yes</u>
244	southward	13 August 2008	40.0° N	26.6° N	<u>yes</u>
245	northward	13 August 2008	40.0° N	24.6° N	<u>yes</u>
246	southward	14 August 2008	40.0° N	25.8° N	<u>no</u>
247	northward	14 August 2008	40.0° N	25.3° N	<u>no</u>
248	southward	10 September 2008	35.5° N	23.5° N	<u>yes</u>
249	northward	10 September 2008	35.5° N	22.7° N	<u>yes</u>
250	southward	11 September 2008	35.5° N	24.9° N	<u>no</u>
251	northward	11 September 2008	35.5° N	24.0° N	<u>no</u>

Xiong, X., Houweling, S., Wei, J., Maddy, E., Sun, F., and Barnett, C.: Methane plume over south Asia during the monsoon season: Satellite observation and model simulation, *Atmos. Chem. Phys.*, 9, 783–794, doi:10.5194/acp-9-783-2009, 2009.

Zahn, A., Brenninkmeijer, C. A. M., Asman, W. A. H., Crutzen, P. J., Heinrich, G., Fischer, H., Cuijpers, J. W. M., and van Velthoven, P. F. J.: Budgets of O₃ and CO in the upper troposphere: CARIBIC passenger aircraft results 1997–2001, *J. Geophys. Res.*, 107, 4337, doi:10.1029/2001JD001529, 2002.

Zahn, A., Weppner, J., Widmann, H., Schlote-Holubek, K., Burger, B., Kühner, T., and Franke, H.: A fast and precise chemiluminescence ozone detector for eddy flux and airborne application, *Atmos. Meas. Tech.*, 5, 363–375, doi:10.5194/amt-5-363-2012, 2012.

Zahn, A., Christner, E., van Velthoven, P. F. J., Rauthe-Schöch, A., and Brenninkmeijer, C. A. M.: Processes controlling water vapor in the upper troposphere / lowermost stratosphere: An analysis of eight years of monthly measurements by the IAGOS-CARIBIC observatory, *J. Geophys. Res.*, 119, 11505–11525, doi:10.1002/2014JD021687, 2014.

Ziereis, H., Schlager, H., Schulte, P., van Velthoven, P. F. J., and Slemr, F.: Distributions of NO, NO_x, and NO_y in the upper troposphere and lower stratosphere between 28° and 61° N during POLINAT 2, *J. Geophys. Res.*, 105, 3653–3664, doi:10.1029/1999JD900870, 2000.

Table 2. Receptor regions used in the analysis of the FLEXPART forward trajectories.

Name	Region
North America	30–50° N, 150–70° W
Central Pacific	10–34° N, 130° E–150° W
Central Africa	0–25° N, 10° W–35° E
Mediterranean	28–40° N, 0° E–40° W
South Asian monsoon	centre: 80° E*, radius: 38° longitude, 16° latitude
TP Stratosphere	higher than thermal tropopause along trajectory
PV Stratosphere	higher than dynamical tropopause (PV > 2.5 PVU) along trajectory

* Latitude of monsoon centre is flight dependent (see [second](#) to last column in Table 1).

Table 3. Slopes of the correlation of NMHC photochemical ages and FLEXPART trajectory transport times for different assumed source regions. The squared Pearson correlation coefficients R^2 are shown in parentheses (see Sect. 3.3.2 for details).

<u>Longitude limit</u>	<u>July</u>	<u>August</u>
<u>80° E</u>	<u>1.12±0.19 (R^2 0.72)</u>	<u>0.91±0.17 (R^2 0.68)</u>
<u>85° E</u>	<u>1.01±0.21 (R^2 0.66)</u>	<u>0.90±0.18 (R^2 0.67)</u>
<u>90° E</u>	<u>1.05±0.25 (R^2 0.63)</u>	<u>0.92±0.18 (R^2 0.69)</u>
<u>95° E</u>	<u>0.97±0.19 (R^2 0.87)</u>	<u>0.93±0.20 (R^2 0.68)</u>
<u>100° E</u>	<u>0.84±0.77 (R^2 0.28)</u>	<u>0.99±0.31 (R^2 0.59)</u>

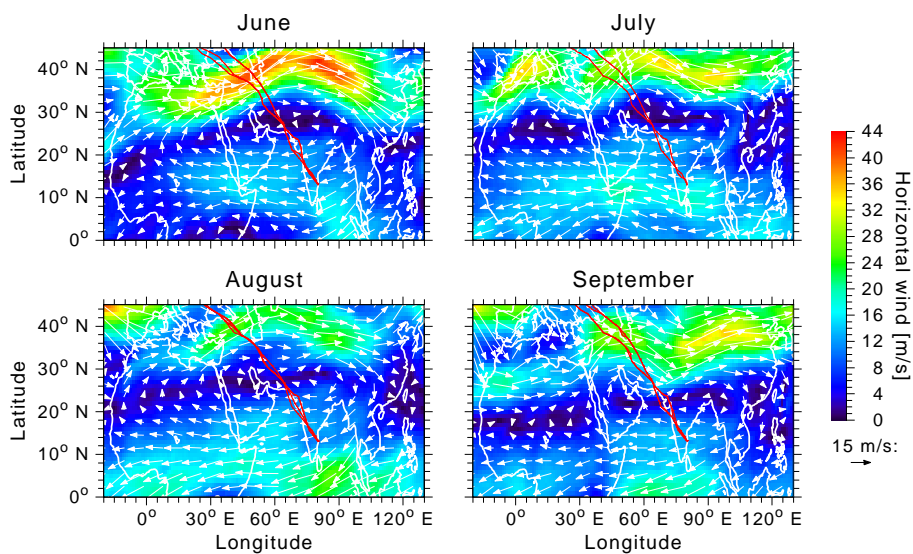


Figure 1. CARIBIC flight tracks across the South Asian monsoon region in June–September 2008. The panels show the flight tracks for each month and 10-day mean ECMWF horizontal wind fields at 250 hPa ending at the day of the last flight in each month. The colour code shows the wind speed while the white arrows indicate the wind direction. Note the anticyclonic monsoon circulation centred over the Indian subcontinent.

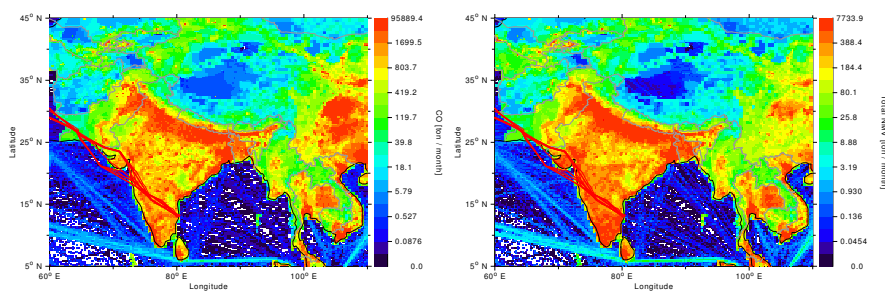


Figure 2. [Emissions of CO \(left panel\)](#) and [non-methane volatile organic compounds \(right panel\)](#) for August 2008 from the [Regional Emission inventory in ASia \(REAS\) v2.1](#) (Kurokawa et al., 2013) including the update from 14 November 2013. The red lines mark the [CARIBIC flight tracks for June to September 2008](#).

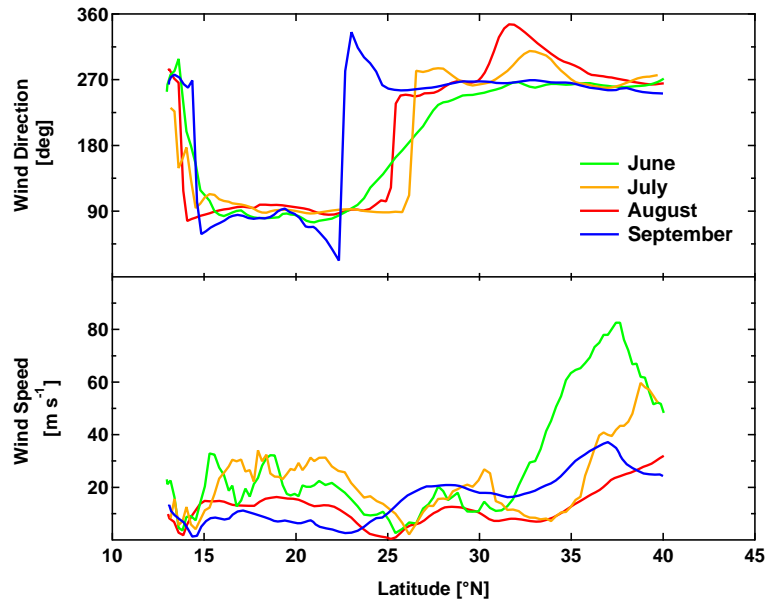


Figure 3. Latitudinal profiles of wind direction (top panel, 90° means wind from the east, 180° from the south, 270° from the west) and wind speed (bottom panel) at aircraft cruise altitude for the first flight from Frankfurt to Chennai in each of the four monsoon months.

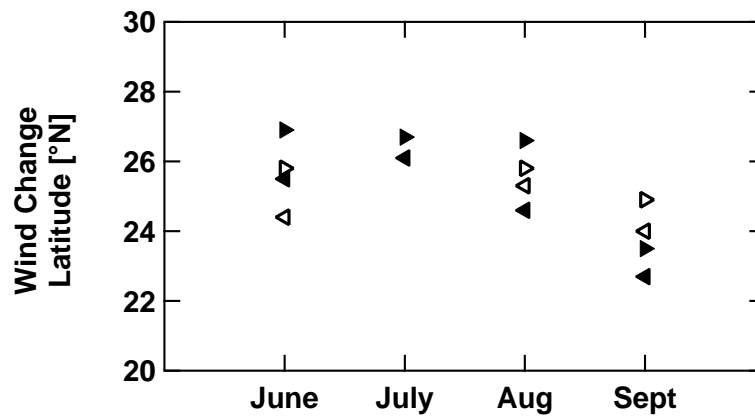


Figure 4. Latitude of the aircraft at the transition between eastward and westward flow in the UTAC for each flight during the summer monsoon 2008. Arrows pointing to the right indicate flights from Frankfurt to Chennai, arrows pointing to the left indicate return flights. Filled symbols represent the first round-trip flight series, open symbols indicate the second (when applicable). For each of the seven pair of flights the wind change (transition point) is about 1° further north on the flight to Chennai (when the aircraft cruise altitude is 1–2 km higher) than on the return flight.

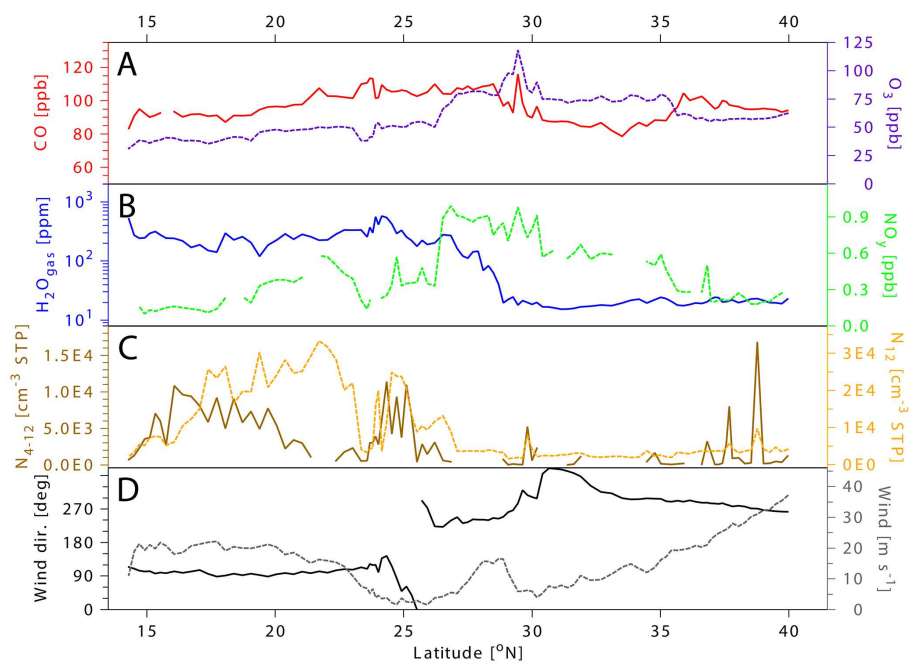


Figure 5. Latitudinal profiles of trace gases and meteorological parameters during the second flight in August from Frankfurt to Chennai on 14 August 2008. In addition to colour-coding of axes, scales for parameters represented by solid lines are on the left and scales for parameters represented by dashed lines are on the right. Aerosol particle number concentrations are given at STP (273.15 K, 1013.25 hPa). Note that all data is shown versus geographical latitude and that the water vapour shown in blue in panel B is on a logarithmic scale (see also Figs. S9–S21).

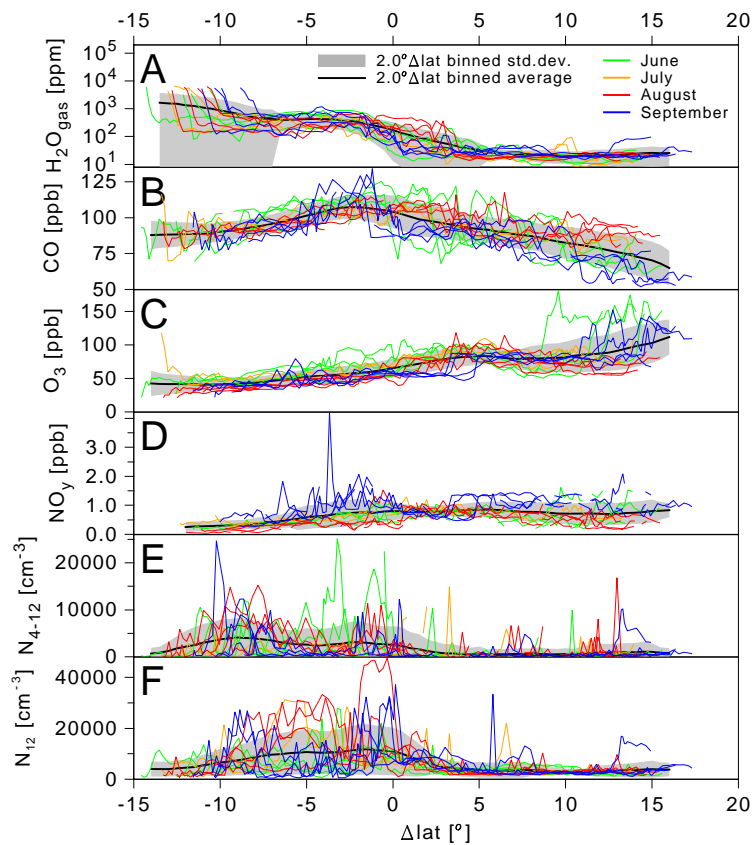


Figure 6. Profiles of trace gases (a-d) (A-D) and aerosol particle number concentrations (e-E and fF), at STP 273.15 K, 1013.25 hPa) vs. relative latitude (Δlat) coordinates for all flights. The colours indicate the first return-flight from Chennai during each month, the black line is the mean over all flights and the grey shading indicates the 1- σ standard deviation around the mean (both calculated over moving 2° Δlat bins). Note the logarithmic scale in the water vapour plot in (a) (see also Figs(A)-S22-S24).

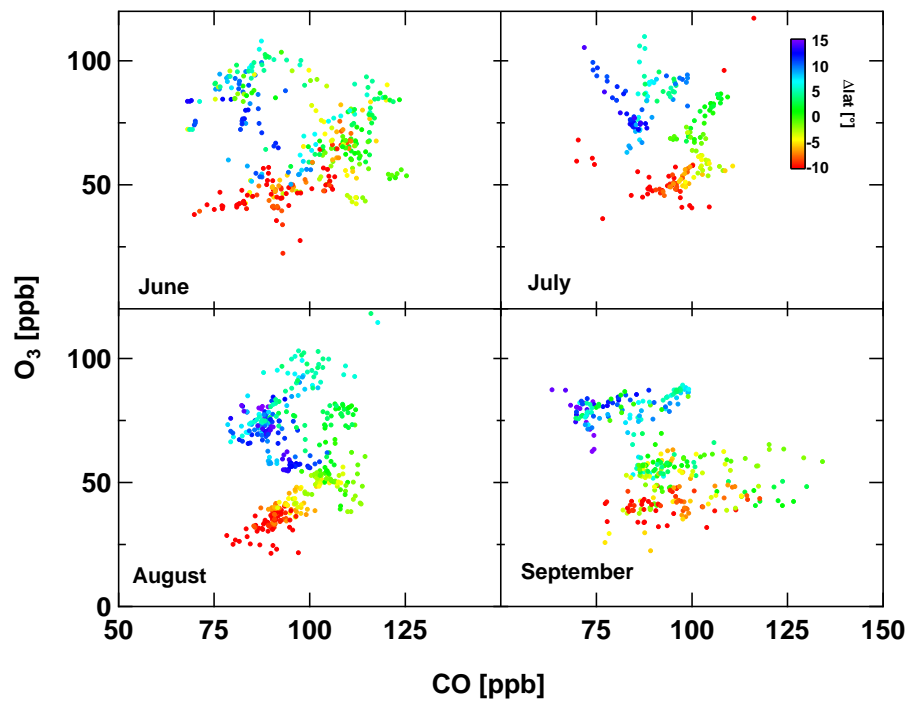


Figure 7. Monthly distributions of O₃ vs. CO during the summer monsoon season 2008. Points are colour-coded by relative position within the UTAC, as determined by Δlat (see also Sect. S6).

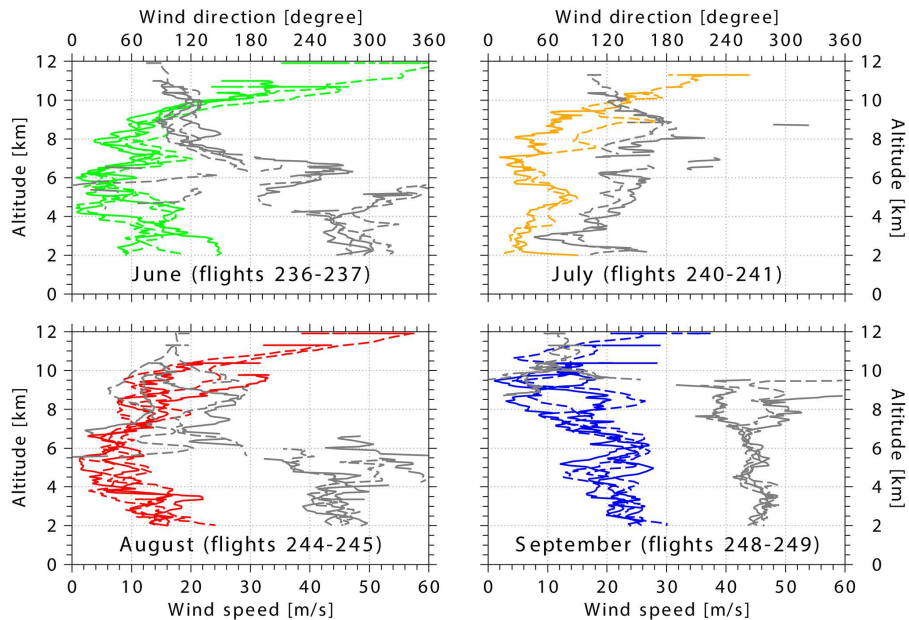


Figure 8. Wind speed (coloured lines, lower x axis) and wind direction (grey lines, upper x axis, 90° means wind from the east, 180° from the south, 270° from the west) from as recorded by the measurements onboard the CARIBIC aircraft for the descent into (solid lines) and ascent from (dashed lines) Chennai. Only data south of 16° N and above 2 km altitude is plotted. Chennai is at 12.99° N, 80.18° E.

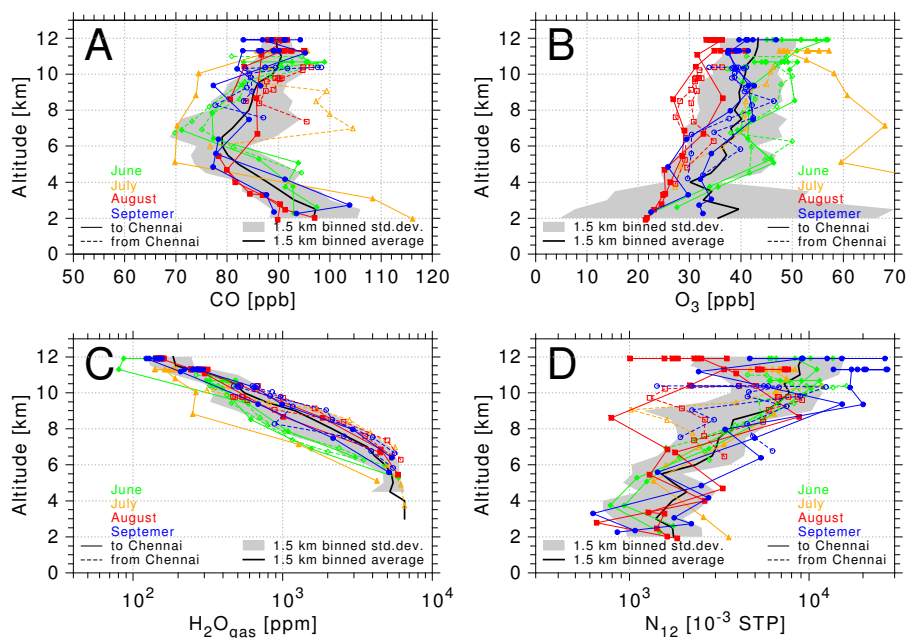


Figure 9. Vertical profiles of CO (a)(A), O₃ (b)(B), water vapour (c)(C) and number concentration of Aitken mode aerosol particles N₁₂ at STP (273.15 K, 1013.25 hPa; dD) between 2 km and 12 km during descent into (solid lines and filled symbols) and ascent from (dashed lines and open symbols) Chennai. The colours indicate the flight month, the black line is the mean over all flights and the grey shading indicates the 1- σ standard deviation around the mean (both calculated over moving 1.5 km altitude bins). Note the logarithmic x axis for water vapour (C) and aerosol particles (D).

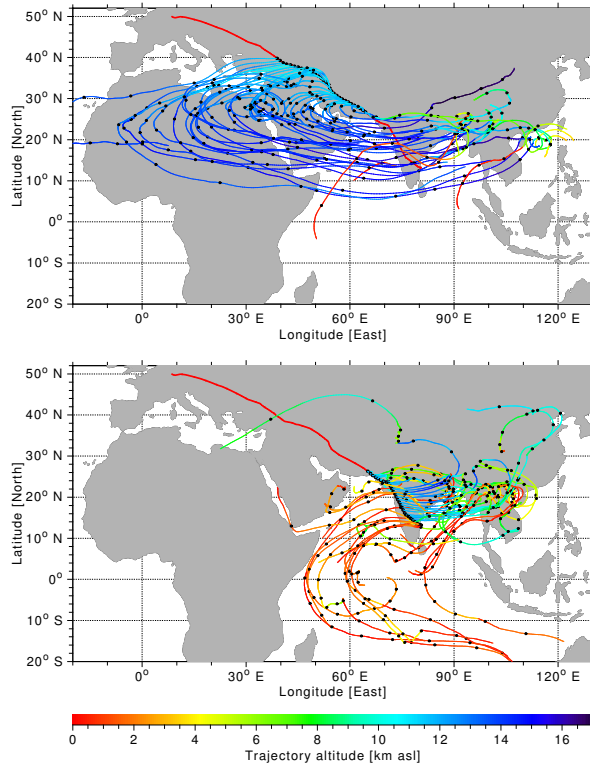


Figure 10. 10 day backward trajectories for CARIBIC flight 244 to Chennai on 13 August 2008. Upper panel: trajectories north of the wind reversal at 26.6° N. Lower panel: trajectories south of the wind reversal. Every second trajectory is plotted for clarity. The colour indicates the trajectory altitude (in km above sea-level) and the black dots mark 24 h time steps along the trajectories. The CARIBIC flight track is shown by the thick red line(see also Figs.-S29–S31):

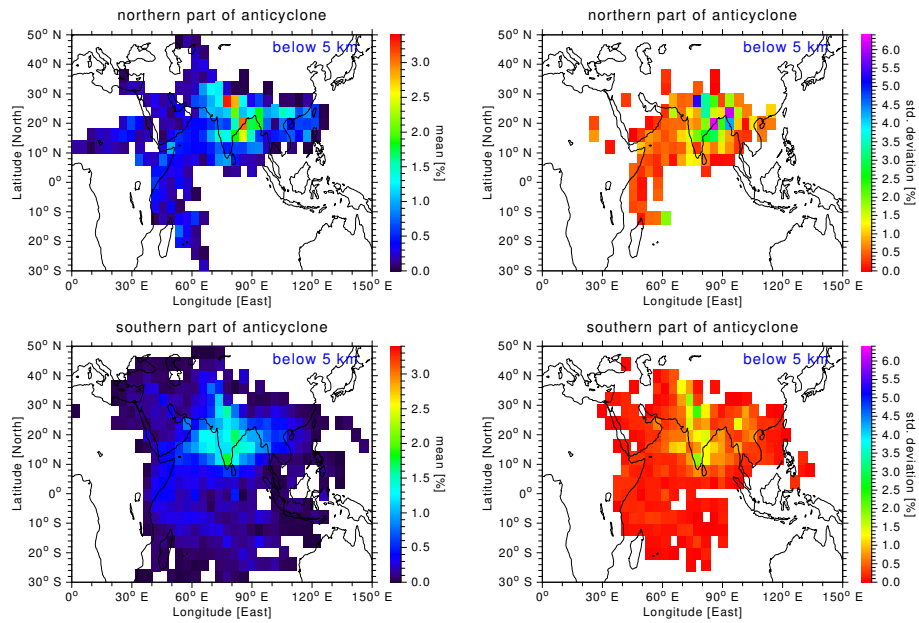


Figure 11. Distribution of source regions for all the CARIBIC flights in August 2008. The colour code shows the percentage of trajectories trajectory points that came from were below 5 km altitude in the preceding 10 days per $4^\circ \times 4^\circ$ grid boxes. Upper left panel: source regions for trajectories starting north of the wind reversal. Lower left panel: source regions for trajectories starting south of the wind reversal. Right panels show the corresponding standard deviation of the percentages in the monsoon months June to September per grid box for all grid boxes reached by trajectories from at least two months (see also Figs. S26–S29).

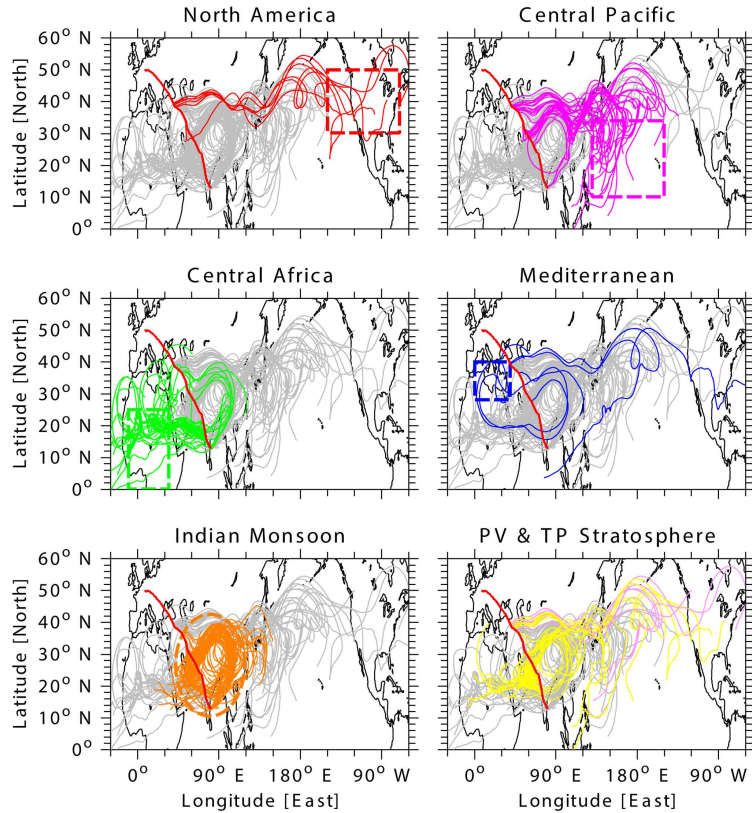


Figure 12. Receptor regions as determined for CARIBIC flight 244 to Chennai on 13 August 2008 (flight track shown with thick red solid line). The panels show all FLEXPART forward trajectories for this flight south of the northern cut-off (40° N) in grey. For each receptor region, the corresponding trajectories are shown in colour. The dashed lines indicate the boundaries of the receptor regions (boxes and ellipse). Trajectories with stratospheric parts are shown in the lower right panel in yellow for the thermal and pink for the dynamical tropopause criterion.

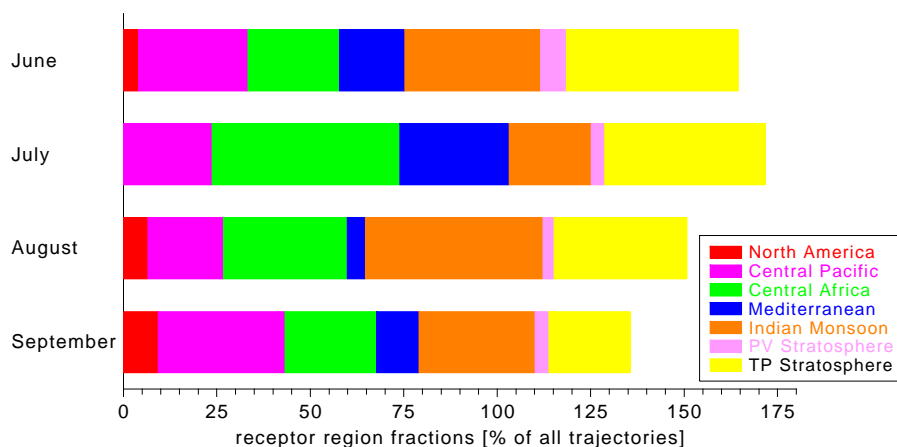


Figure 13. Receptor region fractions averaged over all CARIBIC flights to Chennai in June to September 2008. Since trajectories may reach multiple receptor regions, the totals exceed 100 %.

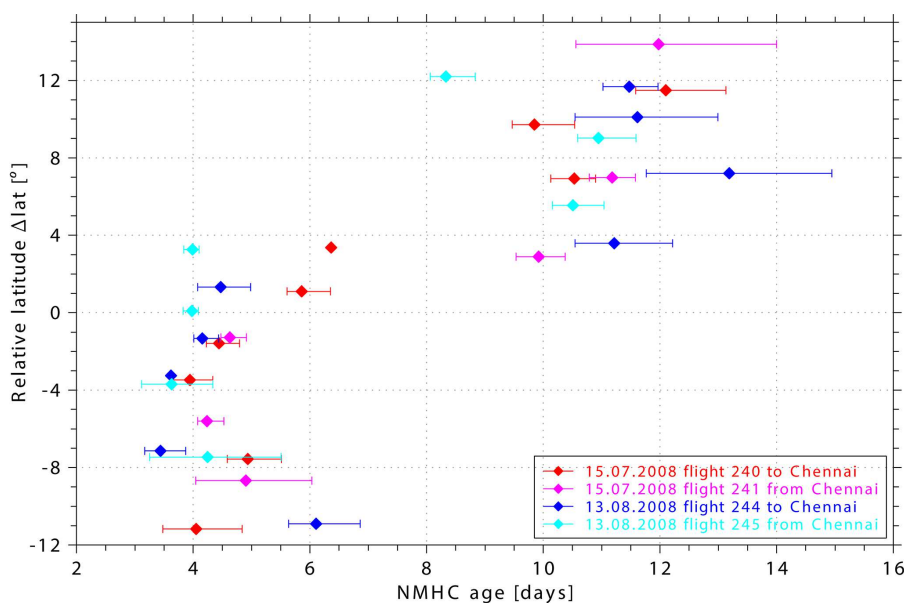


Figure 14. Photochemical age of pollutants in the air samples estimated from NMHC ratios (see Sect. 3.3.2 and Baker et al., 2011) versus relative latitude for the flights in July and the first two flights in August. Note the clustering of the chemically young samples close to and south of the wind reversal ($\Delta\text{lat} \sim 3^\circ$) and the older more chemically processed samples further north. Shown are the mean chemical age together with the minimum and maximum age determined from the propane/ethane, n-butane/ethane and n-butane/propane ratios.

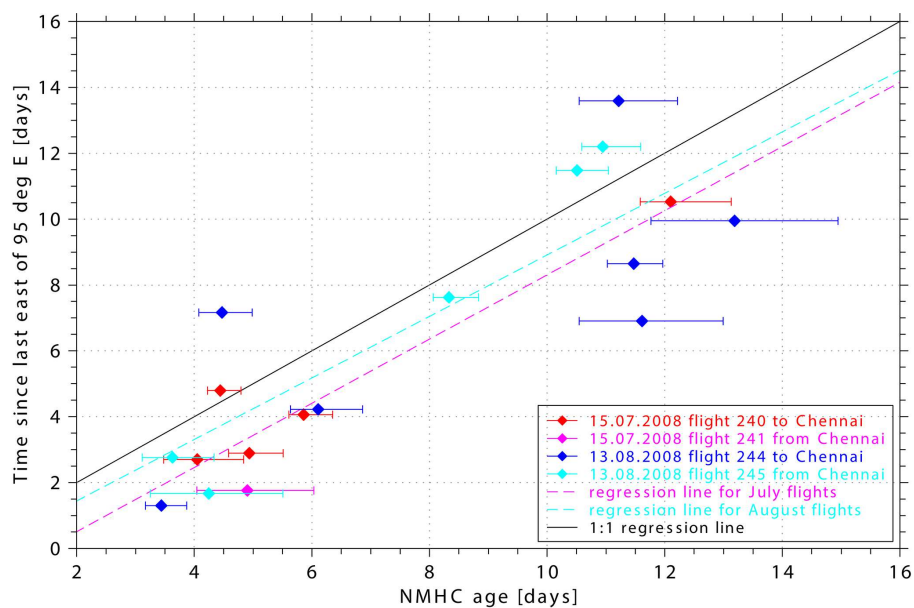


Figure 15. Comparison of the photochemical age of air estimated from NMHC ratios and the time the air had last been east of 95° E according to the FLEXPART trajectory calculations. Shown are the mean chemical age together with the minimum and maximum age determined from the propane/ethane, n-butane/ethane and n-butane/propane ratios. The colours indicate different flights (see legend). The black line indicates perfect agreement of both age estimates while the dashed lines indicate linear least-square regression lines of transport time and chemical ages derived from the different NMHC ratios (magenta regression lines for July, light blue for August flights).

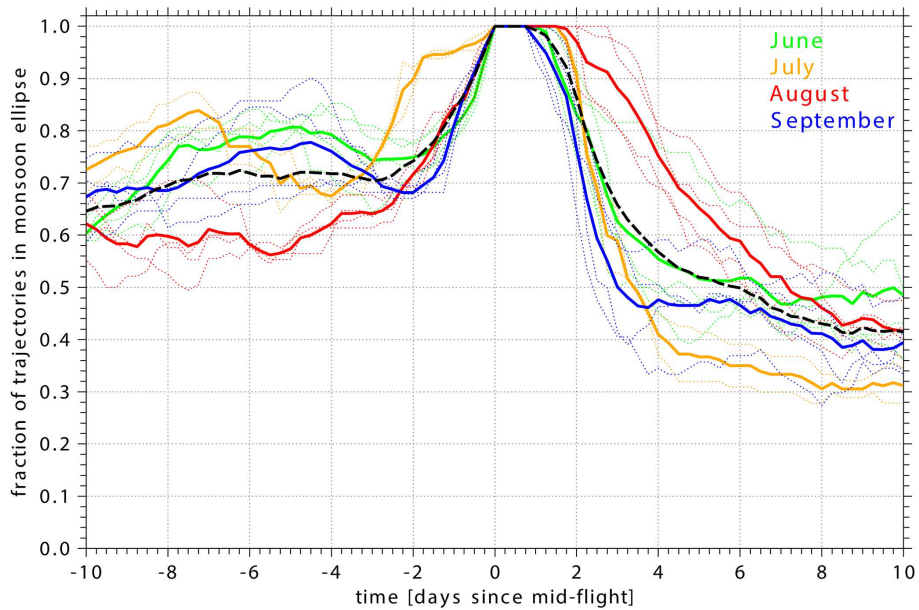


Figure 16. Monsoon leak rates for all flights between June and September 2008. Shown is the fraction of the backward and forward trajectories which started inside the monsoon ellipse ($t = 0$) and are inside the monsoon ellipse at the given time in days before and after the aircraft was inside the monsoon ellipse (see Sect. 3.3.3). The solid coloured lines are monthly means with the results from the single flights indicated by dotted lines. Colours indicate the months. The dashed black line shows the mean leak rate averaged over all flights.